People's Democratic Republic of Algeria
Ministry of Higher Education and Scientific Research
Echahid Hamma Lakhdar University of El Oued
Faculty of Technology
Department of Process Engineering and Petrochemistry

End of study dissertation
In order to obtain the diploma of

ACADEMIC MASTERS

Domain: Science and Technology
Division: Process Engineering
Specialty: Chemical Engineering

Presented by:

- Miss ZOUARI AHMED Zineb
- Miss MITTOU Hend
- Miss BEDOUI Kaouther

Topic

Study and optimization of a process for desalting Algerian crude oil (Case study)

Publicly defended on 27/05/2025 in front of the Jury composed of:

Ms	N. LAMI	Chairman	M.C.B	University of El Oued.
Mr	Y. RADJEB	Examiner	M.C.B	University of El Oued.
Mr	I. BOUDOUH	Supervisor	M.C.A	University of El Oued.

Academic Year: 2024/2025

Acknowledgments

*We extend our sincere thanks and deepest gratitude to **Mr. Issam BOUDOUH**, our academic supervisor at the University of El Oued, for his continuous support and valuable guidance throughout the completion of this work. His constructive feedback and constant encouragement played a significant role in helping us overcome the technical and operational challenges we faced during this experience. We also wish to express our profound appreciation to the esteemed members of the defense committee, especially **Ms. Nassima LAMI**, the principal supervisor, and **Mr. Youcef REDJEB**, the examiner, for dedicating their time to evaluate our work and for their insightful remarks and suggestions, which greatly contributed to its enhancement. Our gratitude extends as well to all the professors of the Faculty of Technology, Process Engineering Department, for their efforts in educating and mentoring us throughout our academic journey. Their dedication has been instrumental in developing our scientific and professional skills, paving the way for a promising future in our field of specialization.*

*We also extend our heartfelt thanks to Engineer **Salah Eddine HANACHI**, our internship supervisor at UTBS, for his valuable guidance, patience, and constant encouragement. His expertise and insightful feedback played a crucial role in deepening our understanding of the practical aspects of crude oil treatment processes.*

*Our sincere appreciation also goes to the entire UTBS team for their warm welcome, professional cooperation, and team spirit. We are especially thankful to Engineer **Abdelatif BELHADEF**, and technicians **Ichrak KARATTA** and **Maissoune OUBIRI** for their technical assistance and collaborative support, which greatly facilitated our integration and task execution.*

*We would also like to thank **Mr. S. TASSINE**, Head of the Field Operation Department at UTBS, for granting us the opportunity to carry out our internship in this key unit and for the trust he placed in us.*

Finally, we express our deep gratitude to our families and friends for their continuous moral support and encouragement, which greatly helped us stay motivated and committed throughout the internship.

This internship has been a valuable and enriching experience, strengthening our passion for the field of crude oil treatment and enabling us to develop essential skills for our professional future.

Dedications

We dedicate this modest work to:
My dear Parents, to whom I owe all the success in my life.
To my dear brothers and sisters
To my family ZOUARI AHMED
To my dear friends
To my colleagues at this job Hend and Kaouther.

ZOUARI AHMED Zineb

My dear Parents who have given me everything, and to whom I owe everything success.
To my dear brothers. To my dear Sisters
To all my family MITTOU
To my dear friends
*To my dear colleagues: Kaouther and Zineb***.**

MITTOU Hend

My dear Parents, to whom I owe all the success in my life.
To my dear brothers and sisters
To all my BEDOUI family
To all my friends
To my dear colleagues: Hend and Zineb.

BEDOUI Kaouther

Abstract

Abstract

This research outlines an approach to assess and improve crude oil desalting based on field measurements, analytical modeling, advanced optimization, and process simulation. Using data obtained from the UTBS's desalting system, inlet and outlet salinities were calculated, and desalting efficiency was determined. A Population Balance Equation model was developed to describe the kinetic nature of salt removal from crude oil, and we selected a customized Differential Evolution (DE) algorithm to reach an efficiency target of 99.00 % under an existing salinity constraint of 40 mg/L. We determined wash-water fraction, the demulsifier addition rate, temperature, and recycle fraction of the UTBS system that achieved 99.00 % desalting efficiency with an outlet salinity of 13.02 mg/L. Aspen HYSYS® simulations corroborated our findings that 70 °C was the temperature that enabled the minimization of residual salinity.

Keywords: crude oil, wash-water, salinity, demulsifier, efficiency, desalting.

Résumé

Cette recherche présente une méthode d'évaluation et de perfectionnement du dessalement du pétrole brut qui repose sur la mesure sur site, la modélisation analytique, l'optimisation avancée et la simulation de procédés. En utilisant les données issues du système de dessalement de l'UTBS, on a calculé les salinités en entrée et en sortie et déterminé l'efficacité du dessalement. Un modèle d'Équation de Bilan de Population a été élaboré pour rendre compte de la nature cinétique de l'élimination du sel du pétrole brut et on a retenu un algorithme d'Évolution Différentielle (DE) sur mesure pour satisfaire un objectif d'efficacité de 99,00 % sous contrainte de salinité de sortie de 40 mg/L. On a déterminé la fraction d'eau de lavage, le taux d'ajout de démulsifiant, la température du système UTBS ainsi que la fraction de recyclage que permettaient d'atteindre une efficacité de dessalage de 99,00 % avec une salinité de sortie de 13,02 mg/L. Les simulations Aspen HYSYS® ont confirmé nos résultats selon lesquels 70 °C était la température qui permettait de minimiser la salinité résiduelle.

Mots-clés : pétrole brut, l'eau de lavage, salinité, démulsifiant, efficacité, dessalement.

ملخص

تحدد هذه الدراسة نهجًا لتقييم وتحسين إزالة الأملاح من النفط الخام استنادًا إلى القياسات الميدانية، والنمذجة التحليلية، والتحسين المتقدم، ومحاكاة العمليات. باستخدام البيانات التي تم الحصول عليها من نظام إزالة الملح في UTBS ، تم حساب ملوحة المدخلات والمخرجات، وتم تحديد كفاءة إزالة الملح. تم تطوير نموذج معادلة توازن سكاني لوصف الطبيعة الحركية لإزالة الملح من النفط الخام، واخترنا خوارزمية التطور التفاضلي (DE) المخصصة لتحقيق هدف كفاءة بنسبة 99 % تحت قيود ملوحة الخروج البالغة 40 ملغ/لتر. حددنا نسبة ماء الغسيل، ومعدل إضافة مادة إزالة الاستحلاب، ودرجة الحرارة، ونسبة إعادة التدوير لنظام UTBS الذي حقق كفاءة إزالة الملح بنسبة 99 % مع ملوحة خارجية تبلغ 13.02 ملغ/لتر. أكدت محاكاة Aspen HYSYS®نتائجنا بأن درجة الحرارة 70 درجة مئوية كانت هي التي تمكنت من تقليل الملوحة المتبقية.

الكلمات المفتاحية: النفط الخام، ماء الغسيل، ملوحة، مادة إزالة الاستحلاب، كفاءة، إزالة الملح.

Table of Contents

Acknowledgments I

Dedications II

Abstract III

Table of Contents V

List of Figures VIII

List of Tables X

List of Abbreviations XI

General Introduction 1

Chapter I: Introduction to Crude Oil Desalting

I-1 Introduction 03

I-2 History of desalting and dehydration 03

I-3 Global trends in crude oil quality 04

I-4 Conventional Method 05

I-4-1 Primary Recovery 05

I-4-2 Secondary Recovery 05

I-4-2-1 Implementation of fluid injection 05

I-5 Nature of salts 06

I-6 Causes of Salt Formation 07

I-7 Disadvantages of salts 07

I-8 Desalination Objectives 07

I-9 Electrostatic Desalter 08

I-10 General Description of the UTBS (Unité de Traitement de Brut Sud) 09

I-10-1 Production Manifold 09

I-10-2 Crude oil stabilization trains 10

I-10-3 Gas compression 11

I-10-4 Oily Water Treatment 11

I-10-5 Off-spec oil system 11

I-10-6 Flare Network 11

I-10-7 Storage Tanks 12

I-11 Description of a UTBS train 12

I-11-1 Reception of crude 12
I-11-2 Crude Oil Processing 13
I-11-2-1 Three-phase separator 14
I-11-2-2 Two-Phase separator 15
I-11-2-3 Desalination Package 15
I-11-2-4 Stabilization Column 17
I-11-2-5 Thermal Stabilization Process in the Reboiler Furnace 18
I-11-2-6 Heat Exchange and Cooling of Stabilized Oil 19
I-11-2-7 Schematic representation of a UTBS train 19
I-12 Description of the electrostatic desalter (VW-21-01) of the UTBS 20
I-12-1 Internal piping 20
I-12-1-1 Emulsion inlet and distribution pipes 21
I-12-1-2 Desalinated crude outlet pipe 21
I-12-1-3 Water drainage pipe 21
I-12-2 Electrodes 21
I-12-3 Transformer-reactor assembly 22
I-12-4 High-voltage power supply assembly 22
I-12-5 Electrical panel and electrical connection 22
I-12-6 Instrumentation 23
I-12-6-1 Mixing valve (21-PV-0X524) 23
I-12-6-2 Interface Level Regulator 23
I-12-6-3 Automatic drainage water valves 24
I-12-7 Accessories and protective equipment 24

Chapter II: Process Design Parameters

II-1 Introduction 25
II-2 Emulsions 25
II-2-1 Emulsion definition 25
II-2-2 Emulsion types 26
II-3 Nature of petroleum emulsions 27
II-3-1 Role of Emulsifying Agents 28
II-3-2 Stability of Emulsions 29
II-3-3 Emulsion Breaking or Demulsification 30
II-4 Factors Affecting Desalting Performance 32

II-4-1 Settling time 32
II-4-2 Chemical or demulsifier injection 33
II-4-3 Heating 34
II-4-4 Dilution with Fresh Water 34
II-4-5 Mixing 35
II-4-6 Electrostatic field 35
II-4-7 pH 37
II-5 Comparison between Desalting Technologies 38
II-5-1 Cameron's Dilectric Technology 38
II-5-2 NATCO's Dual Polarity Technology 39
II-6 Electrical System for Desalters 40
II-6-1 Cameron's dilectric System 41
II-6-2 NATCO's Dual Polarity System 41
II-7 Interface Level Control 42

Chapter III: Practical Application: Monitoring and Calculation of Desalting Efficiency

III-1 Introduction 44
III-2 Determination of Water-Oil Two-Phase Flow Rates 44
III-3 Determination of Process Efficiency 45
III-4 Calculation Results of the Settling Velocity 46
III-5 Settling Time Calculation Results 50
III-6 Residence Time Calculation Results 51
III-7 Sizing of the Desalter 52
III-7-1 Electrical Properties 52
III-7-2 Theoretical and Actual Efficiency of the Desalting System 54
III-7-3- Calculation of the distributor 55
III-8 Modeling and simulation 57
III-8-1 Modeling using Population Balance Equation (PBE) 57
III-8-1-1 Mathematical model 57
III-8-2 Simulation of desalting unit using Aspen HYSYS 63
General conclusion
Bibliographic references
Supplementary Material

List of figures

Chapter I: Introduction to Crude Oil Desalting

Figure I-1:	Types of crude oil	04
Figure I-2:	3D Crystal Structures of Ionic Compounds: NaCl, $MgCl_2$, and $CaCl_2$	06
Figure I-3:	Electrostatic Desalter	08
Figure I-4:	Geographic location of UTBS	09
Figure I-5:	Production manifold	10
Figure I-6:	General operational diagram of UTBS	12
Figure I-7:	The three-phase separator	14
Figure I-8:	The two-phase separator	15
Figure I-9:	Electrostatic desalter	16
Figure I-10:	Stabilization Column	17
Figure I-11:	The furnace	19
Figure I-12:	Process flow diagram of an Algerian oil field (UTBS train)	20

Chapter II: Process Design Parameters

Figure II-1:	Schematic representation of an emulsion: a) Oil in Water, b) Water in Oil	26
Figure II-2:	Emulsion types	27
Figure II-3:	Illustration of demulsification mechanisms. The dark and gray drops refer to the oil and water phases	31
Figure II-4:	Microscopic Representation of Attraction and Coalescence of Water Droplets	36
Figure II-5-a:	Effect of pH and Demulsifier Concentration on Emulsion Stability	37
Figure II-5-b:	Effect of Brine and pH on Emulsion Stability	38
Figure II-6:	Cameron Bilectric® Dehydrator/Desalter	39
Figure II-7:	Temperature requirement vs. API Gravity	40
Figure II-8:	Throughput vs. API Gravity	40
Figure II-9:	AC Electrostatic Coalescer	41
Figure II-10:	Dual Polarity AC/DC Field	42
Figure II-11:	Level Control in the Desalter Using Capacitance Probe	43
Figure II-12:	Level Control in the Desalter Using AGAR System	43

Chapter III: Practical Application: Monitoring and Calculation of Desalting Efficiency

Figure III-1:	Material balance schematic	45
Figure III-2:	variation of the water droplet as a function of water content and washing rate	48
Figure III-3:	Representation of the distance between the electrode and the water phase	52
Figure III-4:	variation of the proportionality coefficient (A') as a function of the washing rate	53
Figure III-5:	Representation of the distributor	55
Figure III-6:	Representative schematic of distributor hole dimensions	56
Figure III-7:	The MATLAB script organigram used for global optimization (Our work)	59
Figure III-8:	Effect of wash water rate on efficiency	60
Figure III-9:	Effect of wash water rate on salinity	60
Figure III-10:	Effect of demulsifier rate on salinity	61
Figure III-11:	Effect of demulsifier rate on efficiency	61
Figure III-12:	Effect of temperature on salinity	62
Figure III-13:	Effect of temperature on efficiency	62
Figure III-14:	Simulated Algerian crude oil desalting unit -Aspen HYSYS V14-	64
Figure III-15:	Relationship between removed salts and Temperature	65

List of tables

Chapter III: Practical Application: Monitoring and Calculation of Desalting Efficiency

Table III.1: Results of the average measurements of water-oil flow rates 44

Table III.2: Flow Rate Results from the Material Balance of the Desalting Unit 45

Table III.3: Process Efficiency Results of the Two Desalters 46

Table III.4: The flow regime and the friction coefficient 47

Table III.5: Determination of water droplet diameter 47

Table III.6: Calculation Results of Crude Oil Viscosity and the Density of the Oil and Water Phases 50

Table III.7: Proportionality coefficient (A') as a function of water content with water content plus washing rate (Y+X) 53

Table III.8: Sub-models for each operational factor on salt removal 58

Table III.9: Optimization results 63

Table III.10: Effect of temperature changes on the process of desalting crude oil 64

List of Abbreviations

Symbol	Definition	Units
Q_c	Crude oil flow rate to be desalted	(m^3/h)
Q_w	Wash water flow rate at the inlet	(m^3/h)
Q_d	Desalted oil flow rate at the inlet	(m^3/h)
$Q_{w'}$	Drain water flow rate	(m^3/h)
Y	The quantity of water injected relative to the crude oil	(% vol)
X	Water cut in the crude oil at the inlet of the desalter	(%)
Z	Water content of the crude oil at the outlet of the desalter	(%)
E_{ff}	The efficiency of the desalting unit	(%)
V_d	Settling velocity	(m/s)
d_d	Density of the dispersed phase	(Kg/m^3)
d_c	Density of the continuous phase	(Kg/m^3)
D	Diameter of water droplets	(m)
g	Acceleration due to gravity	(m/s^2)
Φ	The friction coefficient that depends on the flow regime	(-)
Re	Reynolds number	(-)
D	Droplet diameter	(m)
ϑ	Fluid viscosity	cSt
R	Coefficient de GROSS	(-)
d_{t2}	Density at the given temperature	(Kg/m^3)
d_{t1}	Density at the initial temperature	(Kg/m^3)
α	Coefficient that characterizes the variation of density as a function of temperature	(-)
t_2	Given temperature.	(°C)
t_1	Initial temperature	(°C)
T_d	Settling time	(min)
L_1	Distance between the lower electrode and the interface	(m)
T_s	residence time	(min)
V	volume of the desalter	(m^3)
Q_T	volumetric flow rate of the feed	(m^3/h)
V	Volume of the desalter	(m^3)

V_1	Volume of the cylindrical part of the desalter	(m^3)
V_2	Volume of the two hemispheres	(m^3)
E	The electric field between the electrodes	(V/cm)
U	Voltage of the current	(V)
L	Distance between the electrodes	(cm)
E_1	The electric field between the high water level (interface) and the lower electrode	(V/cm)
L_1	The distance between the high water level and the lower electrode	(cm)
A'	Proportionality coefficient	(-)
E_c	The critical electric field	(V/cm)
Δ	Interfacial tension between water and oil	(g/cm^2)
ε	Dielectric constant	
A	Theoretical optimal salt concentration in the crude oil at the outlet of the desalter	(mg/l)
S_i	Salt concentration in the oil phase at the inlet of the desalter	(mg/l)
S_w	Salt concentration in water dilution (wash water)	(mg/l)
E_{ffT}	Actual efficiency of the desalting system	(%)
E_{Th}	The theoretical efficiency of the desalting process	(%)
L	Distance between the two outermost holes	(mm)
l	Distance between the two ramps	(mm)
n	The number of distribution ramps	(-)
W	Flow velocity	(m/s)
f	Cross-sectional area of a single hole	(m^2)
D	Inner diameter of a hole	(mm)

General Introduction

General Introduction

The global energy consumption continues to rise year after year, pushed by robust economic development and a steadily expanding population. As a result, there has been an almost complete dependence on crude oil as a crucial source of energy and an essential raw material in numerous major sectors, most notably petrochemical industries, transportation, pharmaceuticals, plastics, and paints.

However, crude oil is not pure when it is taken from the ground and contains many contaminants and undesirable chemicals, the most common being water (in emulsions) and inorganic salts, mainly sodium chloride (NaCl), calcium chloride ($CaCl_2$), and magnesium chloride ($MgCl_2$) and then sulfates, silica, iron oxides then some trace metals. These salts are usually dissolved in the water droplets that are dispersed throughout the crude oil, so it is very important to separate the water from crude oil. These impurities are often a primary source of operating problems; for instance, the presence of salts will produce hydrochloric acid (HCl) during the distillation process in the hydrolysis stage, which will be a cause of pipeline and heat exchanger corrosion. Likewise, the accompanying solid particles and metals can clog equipment, which inhibits heat transfer efficiencies with an even greater reduction of the operation of processing units. To mitigate these dangers, desalting is a critical and necessary first step in the crude oil treatment process. Desalting is the process of removing both solid and liquid items before crude is put into distillation units. This technique satisfies numerous critical functions, including:

- Removing chloride salts (Na^+, Ca^{2+}, Mg^{2+}) to protect equipment from rusting.
- Eliminating solid particles and sediments that may hinder flow or cause localized corrosion.
- Preventing the admission of unexpected volumes of water (water slugs) into the distillation unit, thereby ensuring operational stability.

Commercial contractual conditions reinforce the significance of this process, and stipulate the extent of impurities tolerable in crude oil (generally; that is; not more than 40 mg/L of salts and less than 1 % water content). Overall, the three main technologies used in desalting are:

(i) Mechanical desalter- which relies on the density difference between water and oil to facilitate separation by gravity.

(ii) Chemical desalter- uses chemical products called demulsifiers which can enable the breaking of emulsions.

(iii) Electrical desalter- the most used, and involves the use of an electric field to help with the coalescence of fine water droplets and speed the separation process.

This study will involve improving the operating efficiency of the electrostatic desalting unit at the crude oil treatment complex of the UTBS (Unité de Traitement Brut Sud), Hassi Messaoud (HMD). First, daily field data from the UTBS desalting unit are applied to calculate how much crude oil, wash water and drain water are flowing via material balance equations. An estimation of desalting efficiency is made using salinity measurements from the inlet and outlet of the desalter. Next, the basic principles of fluid-dynamics are applied to determine droplet behavior. Settling velocities are calculated using the Stokes' law, criteria for Reynolds numbers are used to validate the laminar regime, then consequent settling times and residence times before settlement were calculated to ensure proper sizing of the equipment. Setting the desalter dimensions and its electrical properties such as sizing distributor holes, inter-electrode electric fields, and critical fields will all help ensure that it operates under an optimal separation performance to satisfy industrial requirements.

Finally, the study used advanced modeling and simulation tools to refine operational parameters related to electrical desalting. A Population Balance Equation model calibrated to salt-removal experimental data was incorporated in a differential-evolution optimization routine in MATLAB to determine with-in salinity limits wash-water fraction, demulsifier rate, temperature and recycle ratio to achieve 99 % desalting efficiency. Parallel Aspen HYSYS (V.14) simulations were used to determine the temperature effects in the salt removal in line with other analytical and computational conclusions.

This research document is organized in the following chapters:

Chapter I: Introduction to Crude Oil Desalting.

Chapter II: Process Design Parameter

Chapter III: Practical Application: Monitoring and Calculation of Desalting Efficiency.

The Master thesis concludes with a global conclusion.

Chapter I

Introduction to Crude Oil Desalting

Introduction to Crude Oil Desalting

I-1 Introduction

Crude oil often contains water, salts, suspended particles, and trace amounts of water-soluble metals. To satisfy these criteria, crude oil's salinity must not exceed 40 mg/L, and the BSW (Basic Sediment and Water) concentration should remain below 1%. Innovative methods and ongoing research are employed to separate salt and water from crude oil. This technique is vital for safeguarding refining and processing facilities while also enhancing the market value of oil barrels.

Desalting, also known as dehydration, is the first stage in refining that removes these contaminants. This technique is critical for decreasing corrosion, clogs, and deposits in equipment. Effective desalting ensures that downstream processing runs smoothly by optimizing water phase removal, dissolving salt crystals in additional water, and then separating the resultant water from crude oil [1].

I-2 History of desalting and dehydration

In the mid-1800s, the need for salt manufacturing in the United States skyrocketed. To obtain salt, the business evaporated subsurface brines. Crude oil was regarded as an unwanted pollutant at the time and frequently accompanied the recovered brine. It was scraped away and thrown. However, the first examination of crude oil at Yale University showed its organic composition, source, and valuable characteristics. This finding piqued the curiosity of petroleum companies, who began to see crude oil; also known as "rock oil"as a significant resource.As a result, the quest for salt halted, paving the stage for a new race to produce oil. This transformation flipped the roles of brine and oil: what was formerly a pollutant became a valuable commodity, while brine became a secondary byproduct. Since then, petroleum technology has improved to accommodate the ever-increasing need for oil while developing more effective extraction techniques [2].

Early oil manufacturing methods were crude, utilizing wooden troughs and basic pipelines. Over time, these methods evolved into complex collection systems, multi-stage separation, and advanced treatment facilities.

Initially, water-in-oil emulsions were handled by allowing the water to settle naturally over time before draining it off. This process was carried out in mechanical devices such as wash tanks. However, it was slow and inefficient, often leaving behind crude oil with a high salt content due to incomplete separation. Alternative methods were needed to improve efficiency and accelerate the process [3].

Heating was later adapted to lower oil viscosity and allow water droplets to settle faster. However, this method had drawbacks: Some water remained retained in the crude oil after mild heating. The hunt for more efficient desalination and dehydration procedures continued. In 1910, a significant breakthrough occurred with the invention of two essential procedures that changed emulsion therapy. The first utilized chemical agents to damage the emulsion coating that surrounds water droplets, allowing for quicker separation. The second breakthrough was applying a high-voltage electrical field to water-in-oil emulsions, causing smaller droplets to mix and enhancing separation efficiency via gravitational forces.

Most industrial facilities now use chemically aided electrical dehydration, a complete process that incorporates chemical demulsifiers, heat, dilution water, mixing, and electrostatic fields to effectively remove water and salts from crude oil [2].

I-3 Global trends in crude oil quality

The InterContinental Exchange (ICE) in London benchmarks North Sea crudes with Brent, while the New York Mercantile Exchange (NYMEX) benchmarks West Texas Intermediate (WTI) for the United States. The graphic below offers a comprehensive summary of the properties that distinguish the various types of crude oil available on the market. Crude oil's quality is determined by its density and sulfur content. Crude oils that are "light" and "sweet" (of extremely high quality) typically cost more than those that are "heavy" and "sour" (of lower quality). This can be explained by the expenses of refining crude oil.The dots on the diagram below reflect the nations as well as the oil's reference names. Colors, on the other hand, represent specific parts of the world (US Energy Information Administration, 2022) [4].

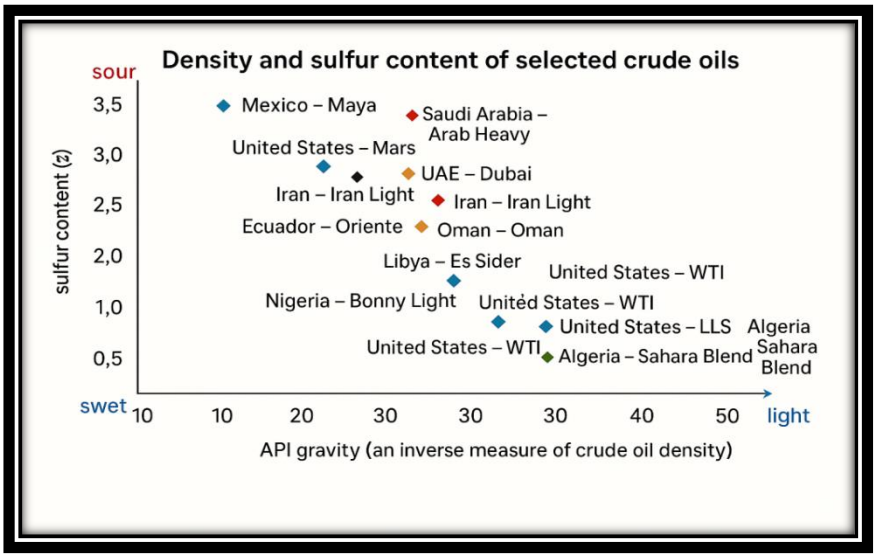

Figure I-1: Types of crude oil

The American Petroleum Institute (API) has established a standard for measuring crude oil in degrees. Here are some relevant facts for categorizing crude oil:

Water: API = 10; an API > 10 floats on water, whereas an API < 10 sinks.

API levels:

- Light (>31.1),
- Medium (22.3-31.1), and heavy (<22.3).
- Extra Heavy: API (< 10.0).

I-4 Conventional Method

I-4-1 Primary Recovery

Primary recovery is the classic method of recovering oil from reservoir rocks with high permeability and porosity. Drilling in the suitable location of the reservoir rock allows the oil to naturally erupt under pressure (passive recovery). If the pressure is insufficient, oil firms will add pumps to increase it. However, current technologies only extract 30% of the crude. As reservoir pressure declines, an extra energy source is needed to bring oil to the surface. Oil firms utilize supplementary procedures known as secondary oil recovery [5].

I-4-2 Secondary Recovery

The flooding method, also known as secondary oil recovery, involves infusing fluids through an injection well system to boost reservoir pressure and displace trapped oil, causing it to flow toward the production well. This method consists of gas injection and water injection (water flooding) (surface water, seawater, and subsurface brine water). The decision is primarily based on technical and economic reasons, while its efficacy is determined by physicochemical parameters and the reservoir's geology. Although more expensive than the main recovery methods, it provides an extra yield of 10 to 15 %. However, secondary recovery is rendered ineffective sooner or later owing to particular variables that result in a considerable volume of oil being retained in the reservoir, known as residual oil. To create more, more sophisticated procedures known as tertiary recovery must be used because up to 60 % of the energy is sometimes lost [5].

I-4-2-1 Implementation of fluid injection

Effective fluid injection into a reservoir necessitates a comprehensive and technically robust approach. This begins with the proper design and equipping of injection wells to ensure controlled and efficient fluid delivery. The injected fluids, whether water or gas, must adhere to stringent standards concerning quantity, quality, and consistency to maintain reservoir integrity

and optimize recovery processes. To meet these standards, the availability of advanced water treatment and pumping facilities, as well as gas treatment and compression systems, is essential. These facilities ensure that the injected fluids are conditioned appropriately for reservoir compatibility. Moreover, the deployment of radioactive tracers is a critical component in monitoring and managing the injection process. These tracers facilitate the tracking of fluid movement within the reservoir, allowing for precise adjustments and ensuring the efficacy of the injection strategy. The integration of these elements is vital for the successful implementation of fluid injection operations in reservoir management [6].

I-5 Nature of salts

In petroleum reservoirs, the extracted fluids generally contain a combination of crude oil, natural gas, and formation water. During production, these components are typically co-produced, with the formation water having dissolved salts that get emulsified inside the crude oil. The major salts contained in crude oil are chlorides, principally sodium chloride (NaCl), magnesium chloride ($MgCl_2$), and calcium chloride ($CaCl_2$). Empirical evidence reveals that sodium chloride contains around 70 % of the total salt content, magnesium chloride about 20 %, and calcium chloride around 10 %. The existence of these salts causes substantial complications throughout the refining process. While sodium chloride is rather stable under refining circumstances, magnesium and calcium chlorides may hydrolyze at high temperatures in the presence of water, creating hydrochloric acid (HCl). This acid is very corrosive and may lead to significant corrosion of refinery equipment. Additionally, the deposition of these salts may induce fouling in heat exchangers and other processing units, limiting efficiency and raising maintenance costs. To address these difficulties, desalting methods are performed to remove the bulk of these salts from crude oil before refining.

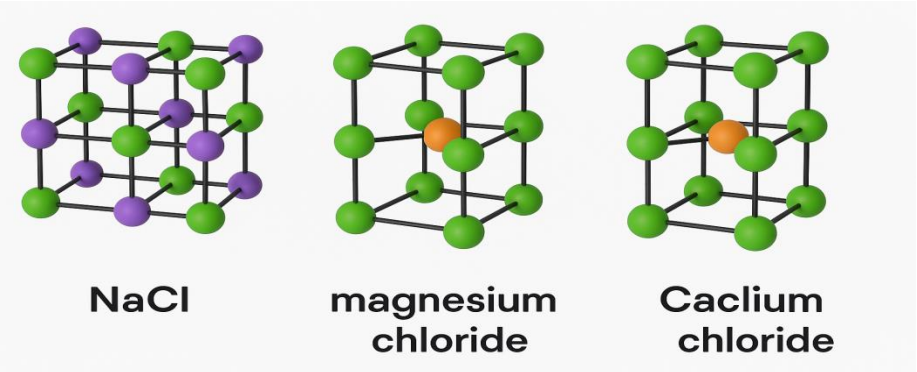

Figure I-2: 3D Crystal Structures of Ionic Compounds: NaCl, $MgCl_2$, and $CaCl_2$.

Salts in crude oil can be crystallized or ionized in water. Ionized salts can be removed by simple decantation. Crystals can be removed with water, which causes them to ionize and hydrate. Hydrated salts are more soluble in water [7].

I-6 Causes of Salt Formation

The presence of salty water in the crude can be caused by a variety of factors [8]:

- Natural causes:

During its travel through the pores of the formation, the oil becomes coupled to the reservoir water, resulting in emulsion. This phenomenon may be insignificant at the start of the exploitation of specific wells, but it gradually presents itself over the life of the oil field.

- Accidental causes:

Emulsified water in crude oil might originate from a zone above the producing layer or casing cement breaking inside the deposit. Injections are used to achieve secondary or tertiary recovery.

- Voluntary causes:

Freshwater washes on production facilities dissolve salt deposits and prepare oil for desalting.

I-7 Disadvantages of salts

Salts present in crude oil pose significant operational challenges in stabilization and topping units of crude processing facilities, where small amounts of inorganic chlorides such as $MgCl_2$ and $CaCl_2$ precipitate upon heating and disrupt downstream operations. These precipitated salts generate fouling layers that restrict the effective flow area inside process equipment, resulting to greater pressure drops and a considerable loss in unit throughput capacity. Furthermore, salt-induced deposits act as thermal insulators on heat exchanger and furnace tube surfaces, substantially diminishing the heat transfer coefficient, impairing thermal efficiency, and necessitating higher fuel consumption to maintain target process temperatures. In parallel, the hydrolysis of chloride salts under process conditions creates aggressive species such as hydrochloric acid, which stimulates under-deposit corrosion and may perforate or rupture exchanger and furnace tubing. Finally, the hydrolysis of inorganic chlorides in the presence of water at extreme temperatures produces both hydrochloric acid and metal hydroxide by-products, further complicating downstream processes and increasing maintenance needs [8].

I-8 Desalination Objectives

In petroleum refining, the removal of dissolved salts is driven by three principal considerations: under certain operational conditions, salts can precipitate as crystalline plates within tubing, pipelines, and treatment equipment, leading to fouling and flow restrictions;

residual chlorides accelerate both electrochemical and chemical corrosion of metal surfaces, undermining equipment integrity and increasing maintenance requirements; and to protect downstream distillation and catalytic units, industry standards mandate that crude oil be treated to reduce chloride content below 40 mg L^{-1}. Consequently, refinery dehydration and desalination processes are implemented to meet these commercial and technical criteria, ensuring uninterrupted production and safeguarding plant assets [9].

I-9 Electrostatic Desalter

In the context of crude oil processing, desalination often entails the use of electrostatic desalters, which are strategically positioned downstream of separators or dehydrators within the processing sequence. These electrostatic desalters are vital for eliminating inorganic salts and residual water from crude oil, therefore minimizing corrosion and fouling in downstream equipment and assuring compliance with product quality requirements. The procedure comprises boiling the crude oil to lower its viscosity, followed by the infusion of wash water to dilute the salt content. Subsequently, the mixture is exposed to a high-voltage electrostatic field inside the desalter unit, facilitating the coalescence of water droplets that encapsulate the dissolved salts. These bigger droplets subsequently sink by gravity, effectively separating from the oil phase. This technology is extensively employed in both upstream and downstream operations because of its effectiveness in boosting the quality of crude oil prior to refining procedures [9].

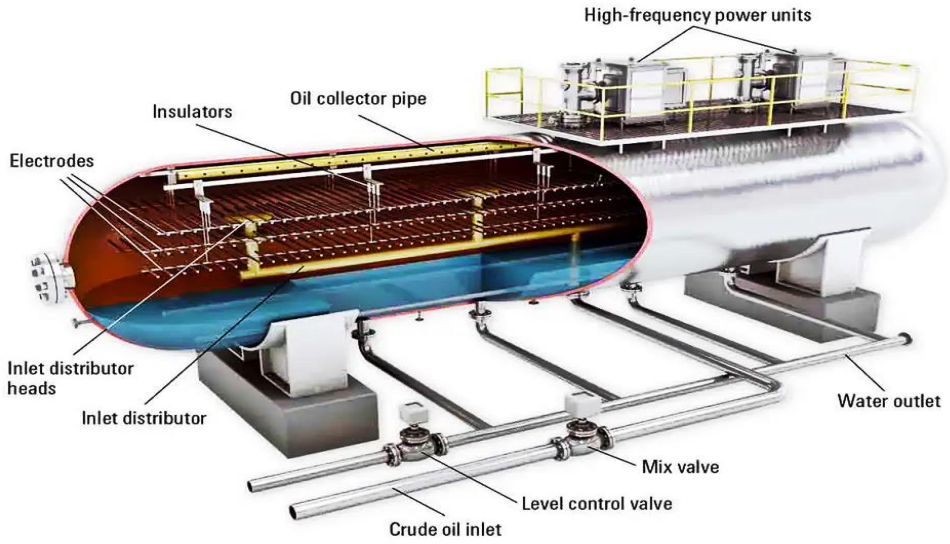

Figure I-3: Electrostatic Desalter

I-10 General Description of the UTBS (Unité de Traitement de Brut Sud) [10].

The UTBS (In French, Unité de Traitement de Brut Sud) was activated in August 2010. So, it is a new crude oil processing unit designed to accept and treat unstabilized oil from six existing satellite fields in the Hassi Messaoud south region, before shipping the stabilized oil to the Haoud El Hamra storage facility.

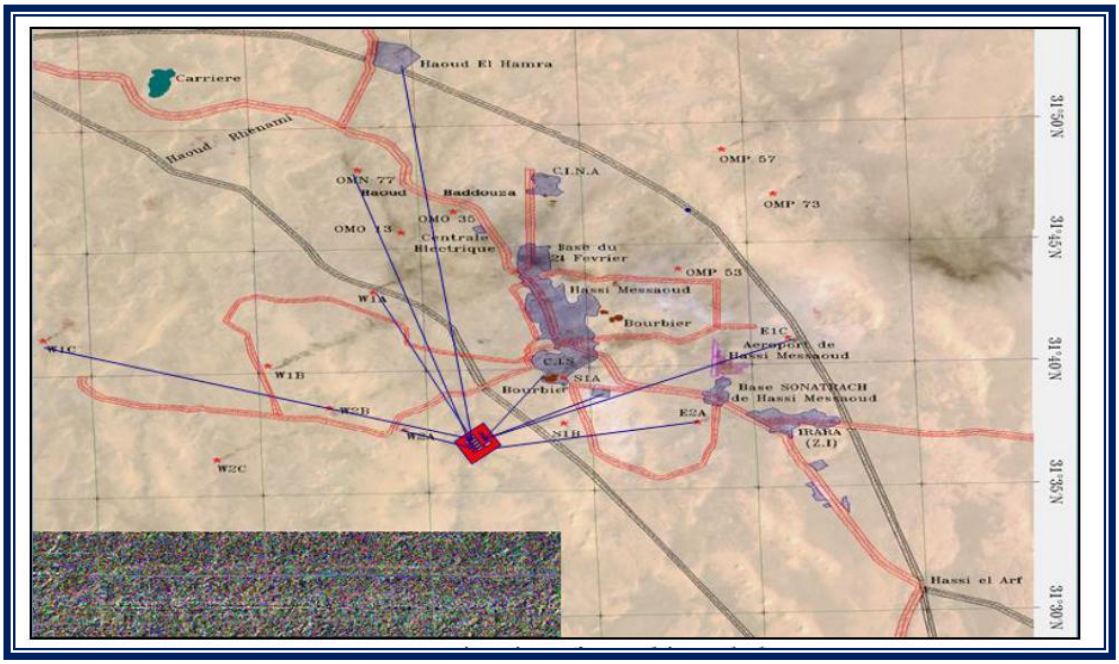

Figure I-4: Geographic location of UTBS

The UTBS includes:

- A production manifold.
- Three crude stabilization trains.
- Four gas compressors.
- A crude oil shipping pump station.
- Utilities (Air/nitrogen plant, oily water treatment, etc.).
- A flare network.
- Storage bins.

I-10-1 Production Manifold

The new collecting network enables the transfer of unstabilized crude from satellites to the M01 manifold.

The MFD M01 contains two collectors:

In the liquid phase, a 24" collector working at a standard pressure of 13.5 bars serves the three oil units as well as the off-spec system in case of surplus. When the oil dispatch pumps of two satellites are out of operation, a second 16" collection operates at low pressure 3 bars in mixed-phase to supply the off-spec system.

Figure I-5: Production manifold

I-10-2 Crude oil stabilization trains

The UTBS consists of three identical oil treatment units, each capable of generating 100,000 barrels per day of stabilized oil.

The three crude oil processing plants fulfill the TVR, salinity, and water content requirements for marketing stabilized crude. The separation of oil, water, and gas occurs in two phases. The first step of separation uses a three-phase separator vessel, whereas the second stage uses a two-phase separator vessel. The desalting package receives oil from the biphasic separator via the desalter feed pumps. The desalination package reduces the BSW content to 0.1% and the salt concentration to 40 mg/l to fulfill marketing criteria.

The desalinated oil feeds the stabilization column, with 20 % of the flow going directly to the top of the column and the other 80 % going to the column's preheater.

The heated stabilized oil exits the column, travels through the preheater on the calender side, and finally via the oil heater, delivering its heat to the unstabilized oil.

Stabilized oil coolers provide ultimate cooling before storage.

The stabilized oil from the three trains is fed into four floating roof storage tanks, each with an effective capacity of 50,000 m^3, via air coolers.

Booster and shipping pumps allow stabilized oil to be sent to HEH via the 30" pipeline installed between UTBS and CIS, and then through the existing 24" pipeline between CIS and HEH.

I-10-3 Gas compression

The flash gas compression system is comprised of four identical compression trains. The gas from the three-phase and two-phase separators and the stabilization columns of the three trains is transported to the flash gas collector, which operates at 4.4 bars. The UTBS uses a portion of the flash gas for fuel, while the surplus is compressed and transferred to the LPG unit at the CIS.

I-10-4 Oily Water Treatment Unit

The oily water treatment package treats oily process water before it is stored in the treated water buffer tank and sent to OMN77 for reinjection into a well or, as a backup, the evaporation pond. The purpose of treating oily water is to lower the amount of hydrocarbons and suspended particulates.

I-10-5 Off-spec oil system

The off-spec oil system is used exceptionally during the startup of the installation or the triggering of one or more oil treatment units (stabilization column, excessively high TVR, etc.).

I-10-6 Flare Network

The objectives of flaring systems are:

- collect all gaseous effluents coming from:

-Temporary unavailability of gas compression facilities and to maintain oil production, gas/oil separators,

- Following an emergency shutdown and then a depressurization of the installations,
- from the voluntary decompression of equipment,
- Consecutive to the opening of one or more safety valves,
- Coming from the gas sky of the equipment maintained under the gas sweep,

- Transfer these effluents from their emission or collection point to the flare-concerned,
- Separate the gases and any potential liquids,
- Burn the gas,
- Recycle the separated liquids back into the process.

I-10-7 Storage Tanks

The oil from the various treatment units is fed into the floating roof storage tanks through the common stabilized oil collector at the air cooler output. An online TVR analyzer may be used to monitor the quality of oil entering into floating roof storage tanks. Four floating roof tanks were installed. Each tank has a usable capacity of 50,000 m³, which is about equivalent to the UTBS's daily production.

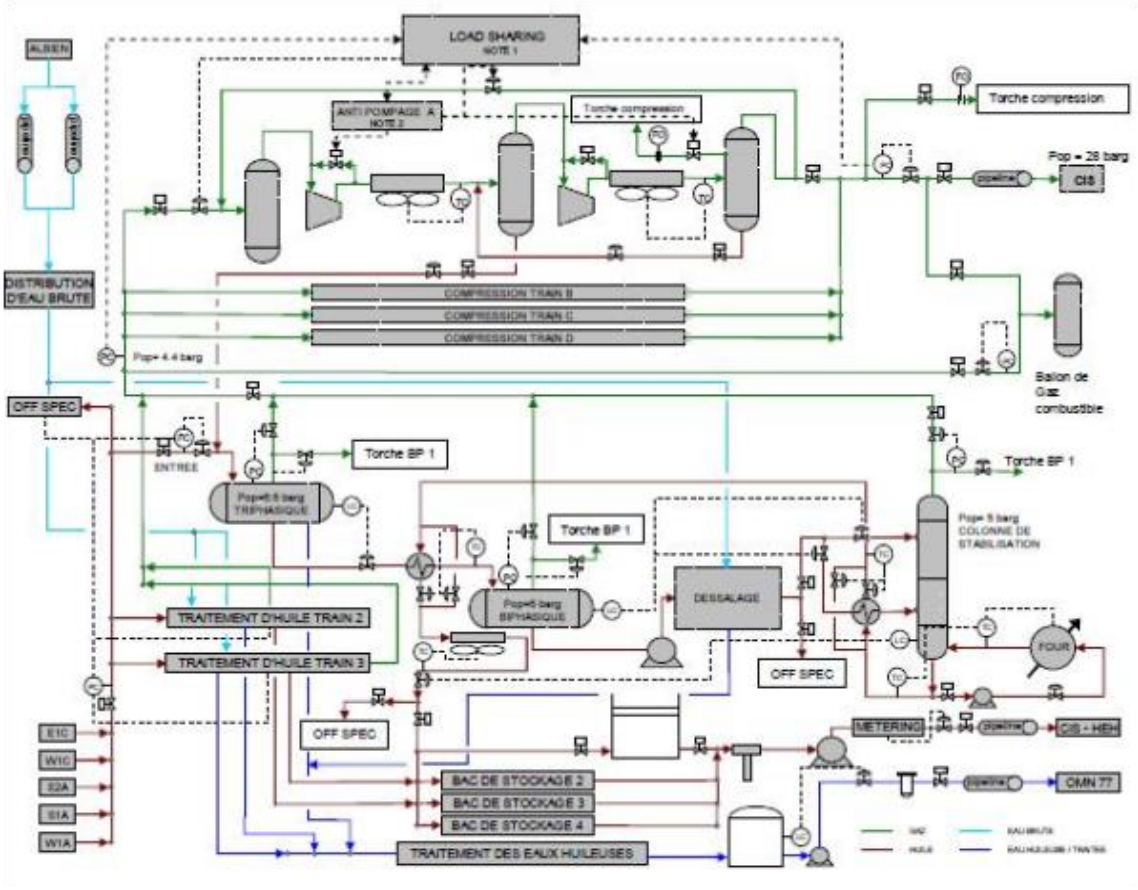

Figure I-6: General operational diagram of UTBS

I-11 Description of a UTBS train [10]

I-11-1 Reception of crude

Producing wells supply the existing satellite platforms where an initial oil/gas/water separation is carried out. At each satellite platform, the unstabilized crude is pumped from the three-phase separator to the existing facilities of the CIS (Southern Industrial Complex) or the new UTBS unit via the new collection network. A set of connections is made to link the existing satellite platforms to the new collection network. The new collection network allows the transportation of unstabilized crude from existing satellite platforms to the M01 manifold located

at the entrance of the UTBS. Crude oil from the satellites can not be stored in floating roof tanks because it can vent.

Three oil processing units with a capacity of 100,000 bbl/day each allow for the transformation of crude oil into stabilized oil that meets export specifications.

To meet these specifications, several steps are necessary:

- First degassing and heating of the oil in the three-phase and two-phase separators and oil heater.
- Desalting performed using two electrostatic separators mounted in series.
- Stabilization of the crude in a stabilization column with upstream oil preheating and reboiling with a furnace.
- Cooling of the stabilized crude oil for storage through the preheaters of the stabilization column, oil heaters, and stabilized oil coolers.

I-11-2 Crude Oil Processing

To store and ship the crude oil, it must meet the following specifications:

- Oil TVR must be compatible with ambient temperature storage, specifically, 7 psi for an outside temperature of 50 °C (in summer) and up to 10 psi for a maximum outside temperature of 25°C (in winter).
- Salinity should be less than or equal to 40 mg/l.
- The insoluble water content in the stabilized crude must be less than or equal to 0.1%.

The three trains of the UTBS are identical and consist of:

- A three-phase separator (PX0-VA-20-01)
- A two-phase separator (PX0-VA-20-02)
- An oil heater (2 calendars PX0-GA-20-01 A/B)
- A desalination package (PX0-UZ-21-01) which includes:

- A first stage of desalination (PX0-VW-21-01)
- A second desalination stage (PX0-VW-21-02)
- Two first-stage water recycling pumps (PX0-PA-21-02 A/B)
- Two second-stage water recycling pumps (PX0-PA-21-03 A/B)

- A stabilization column (PX0-CB-21-01)
- Three reboiler recirculation pumps (PX0-PA-21-01 A/B/C)
- A reboiler (PX0-FA-21-01)

• A stabilized oil refrigerant (3 bays including 2 bundles PX0-GC-21 01A1/A2/B1/B2/C1/C2/D1/D2).

I-11-2-1 Three-phase separator

The three-phase separator (PX0-VA-20-01) constitutes the first stage of water/oil/gas separation. It receives oil directly from the satellites.

The three-phase separator operates at 6.5 bars, with a retention time of 3.7 minutes for the oil and 20 minutes for the water. The gas is sent under pressure control to the compression unit via the gas separation collector, with the excess gas being sent to the unit's low-pressure flare.

The oil, thanks to a level controller, is sent to the oil heater. Considering the low amount of water expected in the crude coming from the satellites where a first separation has already been performed, the water from the process is collected in an appendage called a boot and then sent via a level controller to the oily water treatment unit.

The oil from the three-phase separator passes through the tubes of the oil heater (exchanger) PX0-GA-20-01A/B, chamber side, to be heated to 70 °C, which is the optimal operating temperature of the desalination package. The necessary heat exchange is provided by the stabilized oil heated to 120 °C, coming from the bottom of the column, and passing through the shell side of the exchangers. This provides the necessary heat input for reheating the unstabilized oil (70 °C).

Besides the chambers and tubes, the oil heaters (exchangers) consist of two calenders' in series. Each calendar can be bypassed. The oil heaters (exchangers) PX0-GA-20-01 A/B and the preheaters of the stabilization column PX0-GA-21-01A/B are part of the unit's thermal integration scheme, which allows for the recovery of some of the heat from the hot stabilized oil at the bottom of the column.

Figure I-7: The three-phase separator

I-11-2-2 Two-Phase Separator

The oil heated to 70 °C feeds the two-phase separator (PX0-VA-20-02), which constitutes the second stage of oil/gas separation. It operates at 5 bars with an oil retention time of 3.2 minutes. The flash gas due to heating in the oil heater and the expansion at 5 bars in the two-phase separator is sent to compression via the flash gas collector under pressure control, with the excess gas being sent to the low-pressure flare of the unit. The oil is pumped from the two-phase separator to the desalting package by the desalting feed pumps, and vertical centrifuges, (PX0-PA-20-01 A/B (2 x 100%)).

Figure I-8: The two-phase separator

I-11-2-3 Desalination Package

The desalination package (PX0-UZ-21-01) reduces the BSW content at the package outlet to 0.1% volume and the salt concentration to 20 mg/l equivalent NaCl (desalination design data) to meet the water and salt specifications for stabilized oil during storage (salt concentration below 40 mg/l and BSW below 0.1 % volume guaranteed at UTBS outlet) and to limit column fouling by salt deposits.

The crude-reservoir water mixture is emulsified with recycled wash water from the 1st and 2nd stages of desalination. An emulsion is thus created, thanks to a mixing valve (21-PV-0X524) located upstream of the first stage of the desalination unit (PX0-VW-21-01) and operating at a pressure of 12 bars and 70 °C with a retention time of 5 minutes for oil and 18 minutes for water. This emulsion ensures a good mix between the reservoir water and the wash water, thereby reducing the concentration of salt from the aqueous phase. This emulsion is then separated into two liquid phases in the desalting unit, under the action of an electrostatic field,

which promotes the coalescence of micro water droplets, thus forming larger droplets that fall by gravity to the bottom of the electrostatic separator.

The electrostatic field is created between two electrodes, one connected to the ground and the other connected to a high-voltage transformer installed at the upper part of the desalter. A distributor installed at the entrance of the desalination unit ensures optimal distribution of the oil in the electrostatic field. The coalesced water in the first stage of desalination is sent to the package for oily water treatment. A portion of the water is recycled back to the inlet of the first stage using the first-stage recycling pumps PX0-PA-21-02 A/B (2 x 100%).

The brine exiting the first stage of desalination is then mixed with wash water consisting of a blend of raw water and recirculated water to the second stage of desalination. An effective mixture is recreated thanks to a second mixing valve (21-PV-0X525). Oil and water are once again coalesced in the second stage of the desalting unit (PX0-VW-21-02) operating at a pressure of 10.5 bars and 70°C with a retention time of 5 minutes for the oil and 30 minutes for the water, still under the action of an electrostatic field. The water thus separated in the second desalination stage falls by gravity to the bottom of the separator tank where it is collected, to be largely recycled to the first stage thanks to the recycling pumps of the second stage PX0-PA-21-03 A/B (2 x100%), the rest being sent back to the entrance of the second stage.

An injection of a demulsifier is planned for each desalination stage, upstream of the mixing valve, to facilitate the water/oil separation at each desalination stage.

Figure I-9: Electrostatic desalter

I-11-2-4 Stabilization Column

In the operating configuration of the stabilization column PX0-CB-21-01, desalted crude oil is fed via a bifurcated feed system intended to enhance thermal efficiency and separation performance. Specifically, 20% of the total desalted oil flow is sent as a cold feed to the top of the column, improving early vapor-liquid equilibrium and boosting the removal of light hydrocarbons. The remaining 80% receives preheating via the heat exchangers PX0-GA-21-01 A/B before being delivered into the column as a hot feed. This thermal stratification method guarantees that the bulk of the feed enters at a higher temperature, enabling effective fractionation and lowering the reboiler duty needed for the stabilization process.

The preheater of the stabilization column consists of two calenders in series. The temperature of the oil coming from the desalting package is approximately 70°C.It passes through the tube side. It is heated by the stabilized oil passing through the grille side. To optimize heat recovery, the temperature of the stabilized oil at the outlet of the preheater, on the side calender is regulated to 120 °C.

The stabilization column operating at 5 bars allows for the removal of the lightest compounds from the crude oil and achieves the required TVR at the bottom of the column for storage in floating roof tanks. In other words, the stabilization column allows for increasing the vaporization temperature of the stabilized oil above the outlet temperature of the oil-air coolers. Its operating principle is distillation.

Figure I-10: Stabilization Column

Distillation involves bringing a liquid and vapor into contact at different temperatures. An equilibrium is created between the liquid and the vapor, resulting in an increase in the concentration of light fractions in the gas and an increase in the concentration of heavy fractions in the liquid. The process is repeated on each tray and allows for a separation of the lighter parts of the oil. The heat at the bottom of the column is provided by the reboiler PX0-FA-21-01.

The stabilization column allows achieving a TVR of ~7 psi (in summer), which means obtaining a bubble point of 61 °C at atmospheric pressure, and ~10 psi (in winter), which means obtaining a bubble point of 42 °C at atmospheric pressure.

I-11-2-5 Thermal Stabilization Process in the Reboiler Furnace

A portion of the oil at the bottom of the column feeds the reboiler PX0-FA-21-01 through the reboiler recirculation pumps PX0-PA-21-01 A/B/C (3 x 50%). The furnace provides the necessary heat for stabilization and allows for the vaporization of a portion of the stabilized oil, thereby creating the steam needed for the distillation of the crude.The return to the column of the mixture two-phase at the reboiler outlet is performed below tray 1. The steam feeds tray 1 while the liquid is mixed with the stabilized liquid at the bottom of the column and vaporizes part of it.

The reboiler is a four-pass natural draft furnace. The oil feeding the furnace enters the convection section and flows countercurrent to the flue gases from the radiation section. The convection section includes 3 rows of 8 bare tubes and 5 rows of 8 finned tubes. The fluid then enters the radiation section where it is partially vaporized.

The furnace has six burners and six pilots operating on gas (fuel gas derived from the flash gas of the three-phase and two-phase separators and the stabilization column).The smoke resulting from the combustion of the gas passes through the convection chamber thanks to the natural draft of the chimney adjusted by a manual damper.

Figure I-11: The furnace

I-11-2-6 Heat Exchange and Cooling of Stabilized Oil

The hot stabilized oil (between 135 °C in winter and 160 °C in summer) exits the column and passes through the preheater of the stabilization column on the calender side, then through the oil heater on the calendar side, thus transferring its heat to the unstabilized oil.

The final cooling before storage is ensured by the stabilized oil coolers PX0-GC-21 A/B/C/D, consisting of 4 parallel bays, each bay containing two fans, one of which has variable blades. The oil thus cooled can be sent to the stabilized oil storage tanks or the off-spec oil storage tank.

I-11-2-7 Schematic representation of a UTBS train

The Figure I.11 is a Process Flow Diagram (PFD) illustrating an Algerian oil field's UTBS (Unité de Traitement Brut Sud) processing train. This diagram represents a schematic overview of various interconnected processing units, piping, equipment, and control elements typical of oil production and processing facilities. Different colors and arrows indicate the type and direction of fluid flows:

- Green: Oil flows.
- Yellow: Gas flows.
- Blue: Water flows.

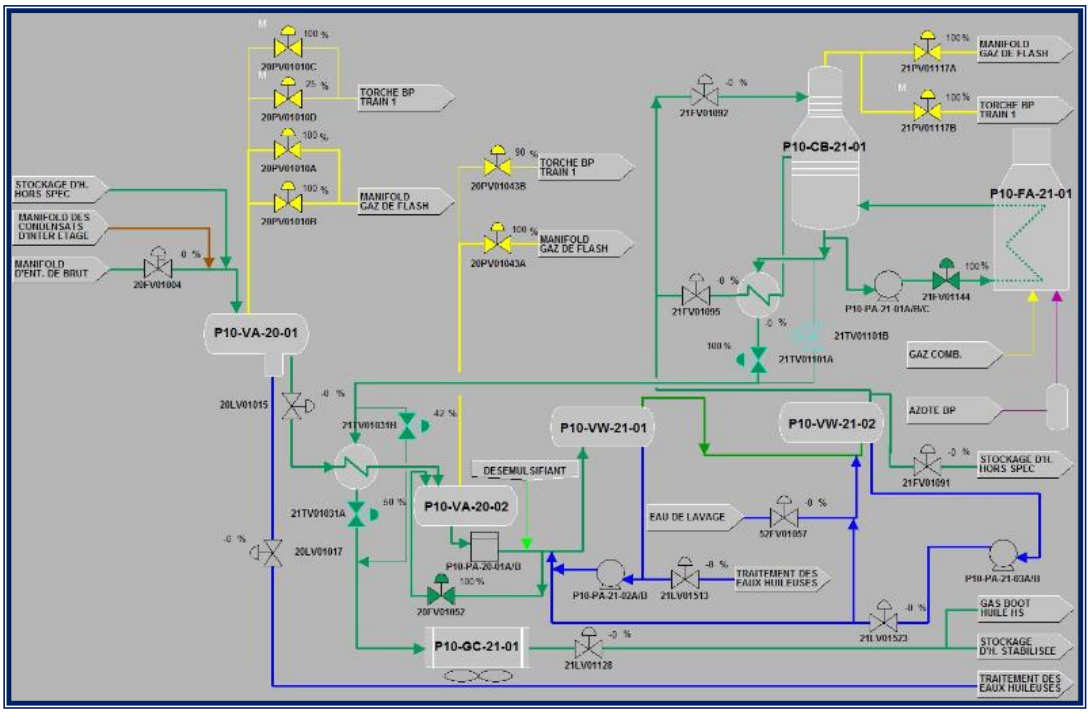

Figure I-12: Process flow diagram of an Algerian oil field (UTBS train)

I-12 Description of the electrostatic desalter (VW-21-01) of the UTBS [7]

The desalter (VW-21-01) of the UTBS in Hassi-Messaoud has the following main characteristics:

- Dimensions: 3000×12000 mm
- Bottom: hemispherical
- Design pressure: 23 bar/vacuum
- Design temperature: -5 /+90 °C
- Material: carbon steel

I-12-1 Internal piping

The internal pipe system of desalination plants is carefully designed to enable the successive phases of the desalination process. Every pair of pipes has a particular purpose, such as moving feed water to pre-treatment units, delivering pressured water to reverse osmosis membranes, or sending brine to disposal systems. The ideal performance and dependability of the desalination plant depend on the effective flow control, pressure control, and integration of many components, which this structured design guarantees.

I-12-1-1 Emulsion inlet and distribution pipes

A horizontally oriented collector is strategically placed in the top portion of the desalter vessel for crude oil desalting operations. Connected directly to four emulsion distributors, this collector uniformly distributes the crude oil-water emulsion throughout the electrostatic field of the desalter. Such a setup guarantees consistent exposure of the emulsion to the electrostatic field, hence promoting the coalescence of water droplets and increasing the general efficiency of the desalting process. Optimal flow dynamics and efficient pollutant removal from the crude oil are provided by the horizontal layout of the collector and its related distributors.

I-12-1-2 Desalinated crude outlet pipe

In the desalting unit of a crude oil processing system, a collector is strategically located in the top portion of the desalter vessel. This collector is oriented parallel to the intake collector and is linked to the output line responsible for delivering the desalinated crude oil. Its principal duty is to assist the effective evacuation of treated oil from the vessel, hence ensuring the continuous flow and operational efficiency of the desalting process.

I-12-1-3 Water drainage pipe

In the crude oil desalting process, a collector pipe is incorporated into the bottom area of the desalter vessel to assist the evacuation of separated water. During desalting, crude oil is heated and blended with wash water, then exposed to an electrostatic field inside the desalter. This field produces coalescence of water droplets floating in the oil, forcing them to combine and sink to the bottom of the vessel owing to gravity. The collector pipe, attached to this lower part, helps to remove the collected water, successfully lowering the salt content in the crude oil and avoiding corrosion and fouling in downstream refinery equipment.

I-12-2 Electrodes

The electrodes crucial to the crude oil desalting unit have been precisely developed to maximize operating efficiency. These electrodes play a vital part in the electrostatic separation process, whereby an electric field is utilized to coalesce water droplets inside the crude oil. This coalescence promotes the separation of water and dissolved salts from the oil, hence minimizing possible corrosion and fouling difficulties in downstream refinery equipment. The design considerations for these electrodes cover issues such as material conductivity, endurance under high-temperature conditions, and ideal geometric layout to provide uniform electric field distribution. By adjusting these parameters, the electrodes contribute considerably to the efficient

removal of salts, thereby assuring the preservation of refinery infrastructure and the creation of high-quality refined products.

I-12-3 Transformer-reactor assembly

In crude oil desalting plants, the transformer-reactor assembly is commonly constructed as an oil-immersed system contained inside a sealed tank. This structure offers good insulation and thermal management, crucial for sustaining operational stability under high-voltage circumstances. The reactor is linked in series with the main circuit, an arrangement that permits the formation of a high-voltage electrostatic field needed for the separation of water and salt contaminants from crude oil. By immersing both the transformer and reactor in insulating oil, the system benefits from higher dielectric strength and efficient heat dissipation, hence boosting the reliability and durability of the desalting process.

I-12-4 High-voltage power supply assembly

In the crude oil desalting process, each transformer-reactor assembly's secondary circuit feeds high-voltage output to electrodes positioned inside the desalter tank. This high-voltage power source is vital for producing the electrostatic field required to remove water and salt contaminants from the crude oil. Typically, the voltage is stepped up from ordinary alternating current (AC) levels to a range between 14,000 and 22,000 volts, employing specialist power units and high-voltage connection assemblies that are authorized for use in hazardous areas. The use of this high-voltage field enhances the coalescence of water droplets inside the oil, boosting the effectiveness of impurity removal.

I-12-5 Electrical panel and electrical connection

The desalination plant situated in Hassi Messaoud (HMD, Algeria) is furnished with a locally produced, explosion-proof electrical control panel, particularly intended to work securely inside hazardous settings typified by the presence of flammable gasses or vapors. This panel is powered by a three-phase electrical supply and comprises various crucial components needed for the unit's performance and safety. These components include cable glands and terminals that enable the electrical supply and create connections between the control panel and transformer-reactor assemblies, as well as interfaces with low-level switches. Additionally, the panel combines an on-off switch coupled to a circuit breaker, indicator lights, voltmeters, and ammeters, all of which are crucial for monitoring and managing the desalination process. The design and construction of this explosion-proof panel adhere to stringent safety standards, ensuring its capability to contain any internal explosions and prevent the ignition of the

surrounding atmosphere, thereby safeguarding both the equipment and personnel in this high-risk operational setting.

I-12-6 Instrumentation

The proper functioning of a crude oil desalination plant depends on the integration of three important instruments: the mixing valve, the interface level regulator, and the automated drainage valve. The mixing valve serves a vital role in achieving comprehensive emulsification by blending heated crude oil with wash water, hence permitting the efficient removal of salts and water-soluble contaminants. Subsequently, the interface level regulator maintains the proper border between the oil and water phases inside the desalter tank, which is critical for increasing separation efficiency and reducing cross-contamination. Finally, the automated drainage valve permits the regulated discharge of the separated aqueous phase, assuring continuous operation and avoiding the buildup of water that may affect the quality of the treated crude oil. Collectively, these components are crucial for ensuring the operational integrity and efficacy of the desalination process in crude oil refining.

I-12-6-1 Mixing valve (21-PV-0X524)

The mixing valve plays a critical role in improving the interaction between salt-laden water droplets and the additional wash water. This valve allows the production of a water-in-oil emulsion, boosting the dissolving of salts into the wash water. Subsequently, the emulsion undergoes separation in an electrostatic desalter, where coalesced water droplets settle off, successfully separating the dissolved salts from the crude oil. The functioning of this mixing valve is normally regulated by a pneumatic actuator, which receives control signals from a regulator located directly on the valve. This arrangement allows for exact control of the mixing strength, guaranteeing excellent desalting efficiency while retaining the integrity of downstream processing equipment.

I-12-6-2 Interface Level Regulator

In crude oil desalting operations, the interface level regulator plays a vital role in regulating the separation of water and oil phases inside the desalter vessel. This regulator supervises the functioning of the pneumatic valve responsible for discharging the aqueous phase, generally referred to as brine. Accurate regulation of the oil-water interface is critical to prevent the carryover of water into the crude oil stream and to avoid oil contamination in the wastewater effluent. Such accuracy is critical for reducing corrosion in downstream equipment and guaranteeing compliance with environmental standards. Advanced measuring methods, including

guided wave radar and radiometric sensors, are applied to identify the interface with great precision, even in tough situations defined by emulsions or variable crude quality. By keeping the interface at an appropriate level, the regulator guarantees effective separation, hence boosting the overall performance and dependability of the desalting process.

I-12-6-3 Automatic drainage water valves

Automated drainage water valves are crucial for ensuring proper separation between oil and water phases inside desalter vessels. These valves work based on input from interface level regulators, which monitor the border between the aqueous and hydrocarbon layers. When the water level rises to a specified threshold, the valve opens to discharge the separated water; conversely, it shuts as the level lowers, so avoiding the unintended loss of hydrocarbons. This automated management is critical for retaining the effectiveness of electrostatic coalescence, a process that depends on a steady interface to successfully remove salts and water from crude oil. Various technologies, including capacitance probes, guided wave radar, and nuclear density profiling systems, are applied to reliably detect interface levels and assure exact valve functioning . Implementing such automated solutions boosts desalter performance, decreases operational disturbances, and lowers the danger of corrosion in downstream refinery equipment.

I-12-7 Accessories and protective equipment

An electrostatic desalter is fitted with several instruments and safety systems to provide effective operation and protection against possible risks. Among its main devices is a thermometer, which measures the inside temperature of the desalter. Maintaining the optimum temperature is critical for improving the separation of water and salts from crude oil, since it determines the effectiveness of the electrostatic coalescence process.

To preserve the system, the desalter contains many protection mechanisms. A safety valve, set to operate at a pressure of 23 bars, avoids overpressure situations that might jeopardize the structural integrity of the vessel. Additionally, a grounding system is built to limit dangers connected with electrical failures, ensuring that any excess current from the transformer is securely diverted to the ground, so safeguarding both equipment and humans. Furthermore, a float switch is put at the top of the tank to monitor liquid levels. This switch performs a key function in avoiding overfilling, which might lead to operational inefficiencies or safety problems. Collectively, these components are important to the safe and efficient working of the electrostatic desalter, assuring both process efficiency and operational safety.

Chapter II

Process Design Parameters

Process Design Parameters

II-1 Introduction

Emulsions are incredibly useful in everyday life because they are used in so many different ways. You can find them in a variety of different things, such food (mayonnaise and milk), cosmetics (lotions and creams), medicines (hormone-based treatments and soluble vitamins), and even agricultural products (herbicide emulsions).

Petroleum-water emulsions are a common and difficult problem in the oil business, both at the production site and in refineries, in addition to these uses. These emulsions can happen on their own during oil field operations or be made on purpose, like when refineries desalinate oil. In either case, the need to break emulsions or improve the separation of oil and water remains a top concern for the economy [11].

This chapter is all about process design parameters. It starts with an introduction and some background information on the subject. It then looks into what petroleum emulsions are like, focusing on the role of emulsifying agents, how stable emulsions are, and how to demulsify them. Next, we look at the several things that can affect the performance of desalting, such as settling time, chemical injection, heating, mixing, adding fresh water, applying electrostatic fields, and pH levels. Next, Cameron's Dielectric Technology and NATCO's Dual Polarity Technology are compared to one other. The chapter then goes into the electrical systems utilized in desalters, with an emphasis on the different systems of Cameron and NATCO. Finally, it tackles interface level control, finishing out the major parts of process design concerns [11].

II-2 Emulsions

II-2-1 Emulsion definition

A more or less stable dispersion of fluid droplets in another immiscible fluid is called an emulsion [12]. As a result, we differentiate between a continuous phase and a scattered phase [13]. Emulsions are classified as either water-in-oil (W/O) or oil-in-water (O/W) emulsions based on the kind of component that disperses in the other [14]. The aqueous phase is the continuous phase of the O/W type, whereas the oily phase is the scattered phase. (The continuous phase is known as the aqueous phase [15]). Figure II-1; displays a real Optical microscopy images of the water and oil emulsions at 400× magnification, acquired by Dr BOUDOUH Issam.

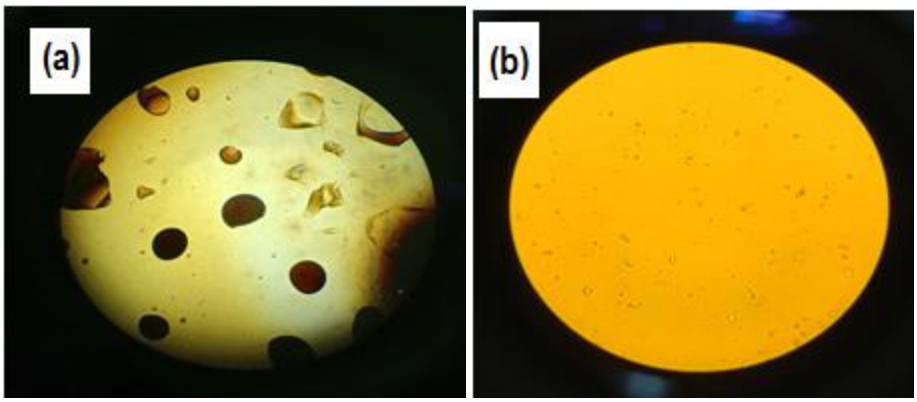

Figure II-1: Optical microscopy images of the water and oil emulsions at 400× magnification: a) Oil in Water, b) Water in Oil. [Our work]

Additionally, emulsions are categorized into three classes according on the size of the dispersed droplets:

(i) Macroemulsions: they are emulsions with droplet sizes ranging from 0.1 to100 μm, these diameters give them a white color [16].

(ii) Microemulsions: their size varies from 100Å to 100 nm. They are often transparent [16, 17].

(iii) Nanoemulsions: referred as emulsions with droplet sizes at the nanoscalenanometric, often from 20 to 200 nm with a transparent or translucent look [18].

An emulsion is frequently formed of two phases: a hydrophilic phase, a lipophilic phase lipophilic and a surfactant:

- The lipophilic phase: sometimes called the fatty phase, oily phase, or organic phase, is generally formed of a range of chemicals from varied sources.
- The hydrophilic phase: also called the aqueous phase primarily includes water and water-soluble compounds.
- Surfactants: they are particularly crucial as they ensure the development and stability of the emulsion over time [19, 20].

II-2-2 Emulsion types

As shown in figure II.2, there are numerous forms of emulsions:

A continuous phase and a dispersed phase make up simple emulsions (a). scattered. When the continuous phase is aqueous (type Oil in Water, O/W), they are known to as direct emulsions; when it is oily (type Water in Oil, W/O), they are referred to as inverses [21].

Multiple emulsions: they are comparable to emulsions within emulsions [22]. These consist of a simple emulsion dispersed throughout a continuous phase. As a consequence, they may be either W/O/W or O/W/O type [21].

Mixed emulsions are emulsions in which the dispersed phase is made up of droplets of various liquid components that vary in concentration or composition. W1+W2/O or O1+O2/W are two potential forms of these emulsions [21].

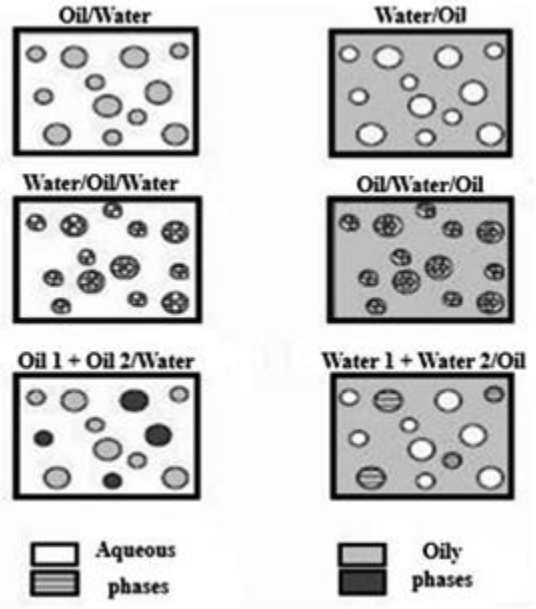

Figure II-2: Emulsion types [22]

II-3 Nature of petroleum emulsions

From the oil reservoirs to transportation, the development of crude oil emulsions is typically witnessed at every step of production. As long as there is adequate blending or an agitator that permits one liquid to disperse as droplets, contact between two immiscible liquids in the presence of an emulsifying agent begins the production of a crude oil emulsion [23]. Numerous studies have demonstrated that the composition of crude oil, which frequently consists of natural emulsifying factors including asphaltenes, acidic chemicals (fatty acid acids, aromatic acid, naphthenic acids), and resins, has a significant impact on the development of crude oil emulsions [24]. Heavy and very heavy crude oils are abundant in these natural emulsifiers.

The authors have showed that various crude oils may have varied emulsion formation and behavior properties. According to a study by Delgado-Linares et al. [25], the natural surfactants in crude oil aid to reduce the oil-water interfacial tension, which in turn stimulates the formation of the interfacial film. This interfacial layer is critical to the emulsion's growth and stability and is differentiated by its mechanical strength [26]. Therefore, the major modifications in emulsification behavior may be impacted by the variance in crude oil compositions. Every natural surfactant has a particular role during the emulsification process. Due to its strong

interfacial activity, asphaltene, which is made up of numerous non-hydrocarbon compounds, contributes in strengthening emulsion stability [27].

Similar to asphaltene, resin is a major component in the production of crude oil emulsion and is made up of a broad array of macromolecular non-hydrocarbon compounds with relatively low molecular weight and polarity [28]. According to Ashrafizadehet al. [29-31], there are numerous techniques for producing oil droplets to generate emulsions, including the use of equipment such as dispersion machines, high shearing stresses, high-pressure homogenizers, and colloid mills. The possibility for automated emulsification by chemical processes or temperature-mediated nucleation processes in one of the phases was also examined by Alwadani [32].

II-3-1 Role of Emulsifying Agents

Water-in-oil emulsions consist of complex combinations of organic and inorganic components. The chemicals that accompany water and oil in these emulsions are known as emulsifying agents, which are surface-active molecules that increase emulsion stability. These agents include asphaltenes (containing sulfur, nitrogen, and oxygen), resins, phenols, organic acids, metallic salts, silt, clays, waxes, and several other components.

Emulsifying agents have varying affinities for oil and water. Some are more drawn to oil, while others have a higher attraction for water droplets. Typically, an emulsifying agent has a molecular structure with two unique parts: a hydrophilic head, which is water-attracting, and a lipophilic tail, which is oil-attracting [11].

In some cases, these agents construct a complex layer at the droplet surface, lowering interfacial tension and generating a robust interfacial film that stabilizes the emulsion. Although emulsifying compounds might be insoluble in either phase, they often concentrate at the interface between oil and water, altering emulsion stability in distinct ways:

(i) Reducing interfacial tension resulted in the creation of smaller water droplets. Smaller droplets are difficult to mix with bigger ones, slowing down separation.

(ii) Creating a physical barrier, generating a viscous covering over droplets that stops them from aggregating.

(iii) Generating electrostatic repulsion, where polar emulsifiers transmit an electrical charge to droplet surfaces, driving them to reject one other and avoid collision and merging.

The kind and concentration of emulsifying agents directly effect emulsion stability. Additionally, temperature history has a significant influence on the production of some

emulsifying agents, notably those connected to paraffins and asphaltenes. Key factors governing emulsion behavior include the degree of interfacial bonding and the pace at which emulsifying agents circulate throughout the system [11].

II-3-2 Stability of Emulsions

The stability of an emulsion, or its ability to be broken, is influenced by several factors:

- **Emulsifier**

This component is important to maintain the stability of an emulsion, since its absence does not guarantee a stable system. The activity of an emulsifying agent is defined by its rate of migration to the interface and its emulsifying capacity [33].

- **Agitation**

The water droplets dispersed in crude oil are influenced by the type and intensity of agitation. Smaller water droplets enhance the stability of the emulsion. From this perspective, measuring the droplet size distribution can be used to assess the stability of an emulsion [33].

- **Crude Oil Viscosity**

The viscosity of the oil phase plays a dual role: on one hand, oil viscosity hinders the migration of the emulsifying agent to the interface and limits the formation of fine droplets due to agitation. On the other hand, high viscosity is an unfavorable factor during the settling of water droplets. In general, both opposing effects are observed [33].

- **Settling and Creaming**

Most crude oil treatment equipment operates on the principle of settling to separate water droplets from oil. Moreover, the friction associated with oil viscosity promotes the movement of water droplets through the oil. This process works only for stable emulsions due to the difference in specific gravity between the components of the emulsion. Settling is accelerated by the thermal treatment of emulsions.

Stokes' law (Equation II.1) provides the settling velocity:

$$V_d = \left[\frac{1}{18}.g\frac{(d_d - d_c)}{d_c}\frac{D^2}{\vartheta_c}\right] \quad \text{(II.1)}$$

With:

g: Acceleration due to gravity (g = 9.81 m/s²)

V_d: Settling velocity (m/s)

d_d: Density of the dispersed phase

d_c: Density of the continuous phase

ν_c: Kinematic viscosity of the crude oil (m^2/s)

D: Diameter of the water droplet (m)

To maximize the settling process, it is required to increase the size of the water droplets and operate at a maximum temperature to minimize the viscosity of the dispersion phase [34].

- **Centrifugation**

This process results in almost complete dehydration and desalting. It is based on the purification of crude oil by adding 8 to 10 % water at temperatures above 80 °C. Centrifugation is governed by Stokes' law, provided that the gravitational force in equation (II.2) is replaced with the equivalent centrifugal force.

$$F = \frac{m.v^2}{R} \quad \text{(II.2.1)}$$

$$V = \frac{2\pi Rn}{60} \quad \text{(II.2.2)}$$

$$F = \left(\frac{2\pi}{60}\right)^2 m.n^2.R^2 \quad \text{(II.2)}$$

Where:

m: Mass of the rotating body (kg)

V: Linear velocity (m/s)

R: Radius of the circle of revolution (m)

n: Rotational speed (rev/s)

According to equation (II.2), it is clear that the centrifugal force is related to the square of the rotational speed [35].

II-3-3 Emulsion Breaking or Demulsification

Numerous components contribute to the demulsification process, which does not happen on its own. These aspects include the interaction of surfactants with the emulsion phases and gravitational forces. The phases involved in chemical demulsification are indicated in Figure II-3.

- **Creaming or sedimentation**

When the dispersed phase has a lower density than the continuous phase, the dispersed phase rises on top of the emulsion. This process is dependent on the size of the droplets (larger droplets will rise if their density is lower than the continuous phase or remain at the bottom if their density is higher). It is also influenced by the rheology of the continuous phase, the hydrodynamic and colloidal interaction between droplets, the electrical charge on the droplets, and the nature of the interfacial membrane or film. As a result, this phenomenon is known as creaming or sedimentation [36].

- **Flocculation**

Flocculation is the process in which the distance between droplets of the dispersed phase reduces owing to the weakening of the net attraction force (Van der Waals) between them, leading the droplets to cluster together without any rupture. The temperature, the oil viscosity, the density differential between the water and the oil, and the water cut all often affect the flocculation rate [37].

- **Coalescence**

Coalescence is the process by which tiny droplets combine to generate larger ones. This procedure reduces the amount of scattered droplets and permits full de-emulsification by removing the thin interfacial coatings that keep them apart. Coalescence is enhanced by elements such as a rapid rate of flocculation, the lack of strong coatings, high interfacial tension, low viscosity, high water cut, and high temperature [37].

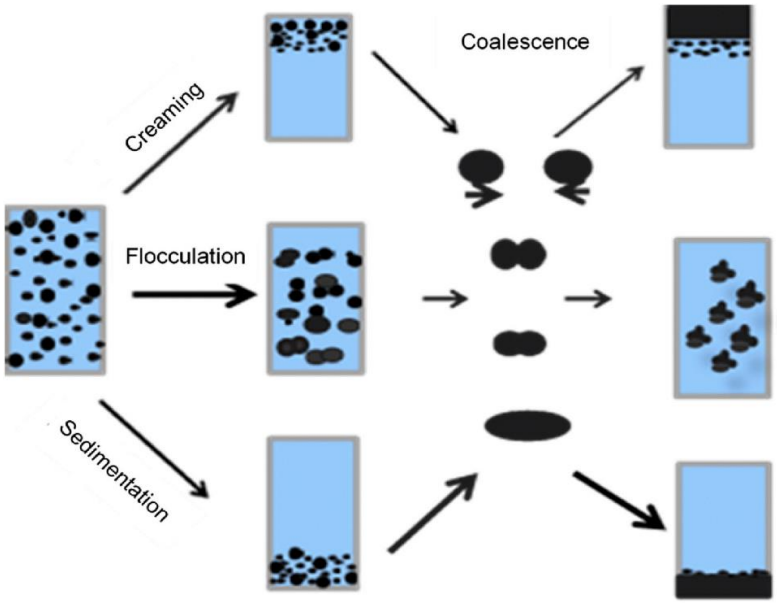

Figure II-3: Demulsification mechanisms (The dark and gray drops refer to the oil and water phases)

II-4 Factors Affecting Desalting Performance

The treatment of emulsions essentially includes enabling water droplets to settle and be drained off. This procedure takes place in wash tanks, separators, and desalting vessels. However, to hasten settling and enhance efficiency, numerous strategies may be employed:

- **Injection of demulsifiers** – Chemical agents that break the emulsion and promote water separation.
- **Application of heat** – Reduces oil viscosity, facilitating water droplet coalescence.
- **Addition of fresh water** – Dilutes emulsions, making separation easier.
- **Application of electricity** – Electrostatic fields enhance droplet coalescence.

The primary objective of a desalting plant is to break the protective films around water droplets, enable them to merge into larger drops and ensure efficient water separation. Several key factors influence the performance of a desalting process, including:

II-4-1 Settling time

The desalting process employs one or more of the previously mentioned procedures to increase the water weight, thereby accelerating its settling and drainage. Consequently, gravity differential serves as the fundamental scientific principle underlying all emulsion treatment plants.

Formation water can flow with crude oil in two forms: free and emulsified. Free water is not intimately mixed with the crude; instead, it exists as larger droplets dispersed throughout the oil phase. This type of water is easily removable using gravity-based oil-water separators, surge tanks (wet tanks), and desalting vessels [11].

In contrast, emulsified water is finely dispersed as tiny droplets within the oil phase, making it difficult to remove with simple settling devices. Therefore, additional treatment methods such as chemical injection, freshwater dilution, mixing, heating, and electrical treatment are required.

The desalting process primarily relies on gravity to separate water droplets from the continuous oil phase. However, a drag force opposing gravity is exerted as water droplets move downward through the oil. Thus, adequate design considerations must be incorporated into the desalting and dehydration system to enhance gravitational separation [11].

Gravitational residence time is determined based on Stokes' equation as follows:

$$\nu = \frac{2\pi r^2(\Delta\rho)g}{9\eta} \quad \text{(II.3)}$$

Where:

ν: is the downward velocity of the water droplet with radius r.

Δρ: represents the density difference between the two phases.

η: is the viscosity of the oil phase.

This equation suggests that gravitational separation can be optimized by:

- Maximizing the size of coalesced water droplets.
- Increasing the density difference between water droplets and the oil phase.
- Reducing the viscosity of the oil phase.

Factors (2) and (3) can be best achieved through heating and the addition of dilution water (fresh water), while the application of an electric field enhances factor (1) [11].

II-4-2 Chemical or demulsifier injection

Emulsions may be further treated by introducing chemical destabilizers. These surface-active chemicals adsorb to the water-oil interface, fracturing the layer covering the water droplets and driving the emulsifying agents back into the oil. Once the covering is broken, water droplets may collide spontaneously due to molecular attraction forces.

For chemical injection to be effective, the chemical must be able to dissolve in the surface layer surrounding the water droplets. Additionally, it should consist of polar molecules that are attracted to the acidic or organic skins surrounding the water droplets, which are likewise made of polar components. Emulsifying chemicals produce a thin protective covering around water droplets, preventing them from mixing. These coatings consist of polar molecules, causing the interaction between water droplets analogous to that of two bar magnets being drawn together [11].

A demulsifier interacts with the emulsifying agent or the protective layer, weakening or breaking it. Time and turbulence help the demulsifier penetrate through the oil to the interface. Once the demulsifier has broken the natural protective covering, it reveals a thinner layer that is more prone to rupture by water-to-water attraction forces at very close distances.

The calculations for chemical/demulsifier application are based on three key assumptions:

- The continuous phase is oil.
- The chemical (demulsifier) acts and travels within the continuous phase.
- The demulsifier is insoluble in water but soluble in oil.

The lower the water content in an emulsion, the more challenging it is to treat. This is due to the following factors:

- The distribution of water droplets in the continuous phase depends on the water content. As the water percentage increases, water droplets become closer together.
- A lower water percentage results in a higher concentration of emulsifying agents at the water-oil interface.
- Dispersed water droplets are more difficult to coalesce than those in close proximity. Additionally, the rate of coalescence depends on the droplet radius.

II-4-3 Heating

The layer that surrounds water droplets becomes less cohesive, thick, and viscous when heated. Additionally, heat lowers the viscosity of the continuous phase (oil), which facilitates the free and quick movement of water droplets during coalescence. Maintaining temperature control throughout operations is an extremely difficult task. Excessive heat can promote evaporation, which lowers the API gravity and lowers the price in addition to reducing the volume of oil [38].

Generally speaking, liquid density and viscosity decrease with temperature. The settling rate will increase as the operation temperature rises, improving separation in the process. An increase in separation efficiency allows for the simultaneous desalting of a greater volume of oil. According to this, it would be more convenient to have a greater temperature. The conductivity of crude oil, however, rises with temperature, as does the process's power needs. Temperature increases also mean greater heating expenses. There must be an ideal temperature in light of these conflicting data [39].

II-4-4 Dilution with fresh water

Despite reduced demulsifier quantity and operating temperature values, it is clear that the volume of wash water directly correlates with the amount of salt removed from crude oil [40]. Emulsion salts can occasionally be solid crystals. As a result, freshwater is required to dissolve

these crystal salts, and desalting and dehydration procedures now require freshwater dilution. To improve mixing efficiency and avoid scaling inside pipes and heating tubes, freshwater is typically injected before to heat exchangers. To wash away and subsequently drain off water droplets in emulsions, freshwater is injected. Thus, the phrase "wash water". In general, the injection rate is 3–10 % of the total crude flow, while the amount or ratio of freshwater injected depends on the petroleum's API gravity. The wash water injection needs to be run at its peak efficiency to increase W/C efficiency. After that, too much water can cause the pH range of the entire water volume to deteriorate, according to experience. Significant issues with emulsion breaking and the precipitation of hydrocarbon particles (like naphthalene) into the continuous water phase might arise from pH ranges above or below 7 [38].

II-4-5 Mixing

In the desalting/dehydration process, mixing is utilized to encourage the dilution water and demulsifier to further disperse with the emulsion. Additionally, it aids in the coalescence of smaller water droplets, which improves the salts removal efficiency (S/R) and specifically impacts water cut dehydration efficiency (W/C). Emulsions are created by high-shear actions. Similar to this, dilution water, or freshwater, must be mixed with an emulsion to dissolve the salt crystal and help the finely dispersed droplets coalesce [38].

The mixing process involves three steps: joining smaller droplets, blending emulsions with a chemical or demulsifier, and uniformly dispersing wash water into emulsion-sized drops.

II-4-6 Electrostatic field

The applied electrical voltage gradient significantly impacts desalting efficiency. However, this parameter is determined during the design phase, as the transformer supplies a constant voltage to the electrical grid, and modifying the arrangement of electrical grids inside the desalter vessel is not easily feasible.

Within the desalter vessel, water droplets in the emulsion possess both positively and negatively charged ends. The electrical grid distorts these originally spherical droplets into more elliptical shapes. Depending on their internal charges and positioning within the desalter, the droplets are attracted to either the positive or negative electrodes, facilitating their separation. The positive end of one droplet will be close to the negative end of another droplet, thus providing an electrostatic attraction [41]. This is illustrated in Figure II-4.

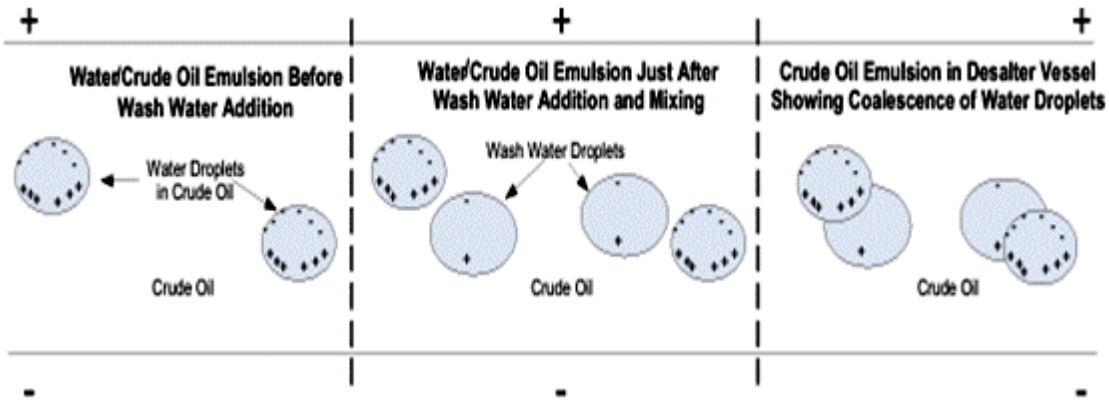

Figure II-4: Microscopic representation of attraction and coalescence of water droplets [41]

The electrostatic attraction between droplets can be represented by the following equation (II.4):

$$F = \frac{KE^2 d^6}{S^4} \tag{II.4}$$

Where:

F: Electrostatic force between two adjacent droplets (N).

E: Voltage gradient (V/m).

K: Dielectric constant for crude oil-water system.

D: Diameter of water droplets.

S: Centre-to-centre distance between two adjacent droplets.

As demonstrated in Equation (II.4), raising the voltage gradient improves the electrostatic force between nearby water droplets, enhancing separation efficiency. However, there are various restrictions to raising the voltage gradient.

First, transformers can only offer a set voltage to the electrical networks. While several transformers might be constructed to enhance the voltage, the initial capital cost may exceed the economic gains received from better separation efficiency. Second, below a specific voltage threshold, water droplets begin to break, generating smaller droplets. These smaller droplets display stronger interfacial tension, leading to a more stable emulsion. This event happens at the critical voltage gradient, as given by Equation (II.5) [33].

$$E_C = k\sqrt{\frac{T}{d}} \tag{II.5}$$

Where:

E_C: Critical voltage gradient (V/m)

K: Dielectric constant for crude oil-water system

T: Surface tension

d: Diameter of droplet

As shown in Equation (II.5), the critical voltage gradient decreases as the droplet diameter increases. Therefore, the critical voltage gradient must be determined based on the expected droplet diameter at the point where sufficient coalescence has occurred for the water droplets to settle out of the oil phase.

II-4-7 pH

Crude oil contains a number of organic acids and bases that act as emulsifiers by modifying surface charges at the oil/water interface [42]. The ionizability of these components is influenced by the emulsion's pH, which can significantly impact the physical structure of the emulsion and, consequently, its stability. Fortunately, the addition of a demulsifier can greatly broaden the range of pH over which successful separation can be achieved [43].

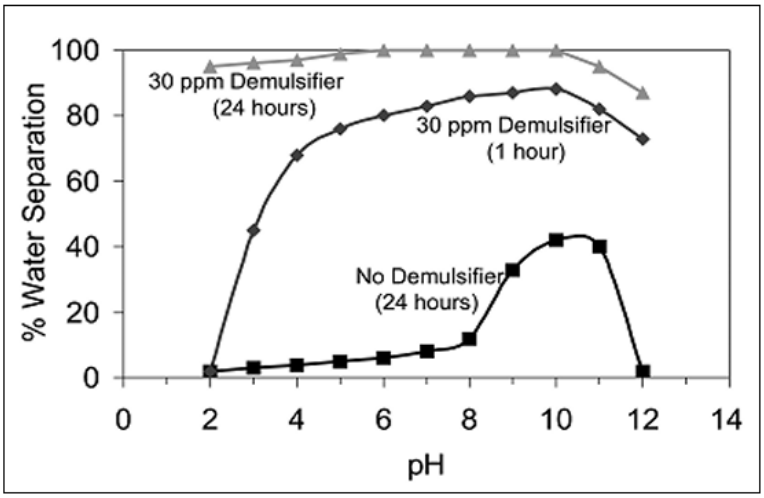

Figure II-5-a: Effect of pH and demulsifier concentration on emulsion stability [43]

The composition of the water phase also plays a significant role in emulsion stability. Ionic interactions between salts and the acids and bases at the oil-water interface . Higher concentrations of brine in the water phase lower the optimal pH for separation and broaden the overall peak, as illustrated in Figure II-5-a [43].

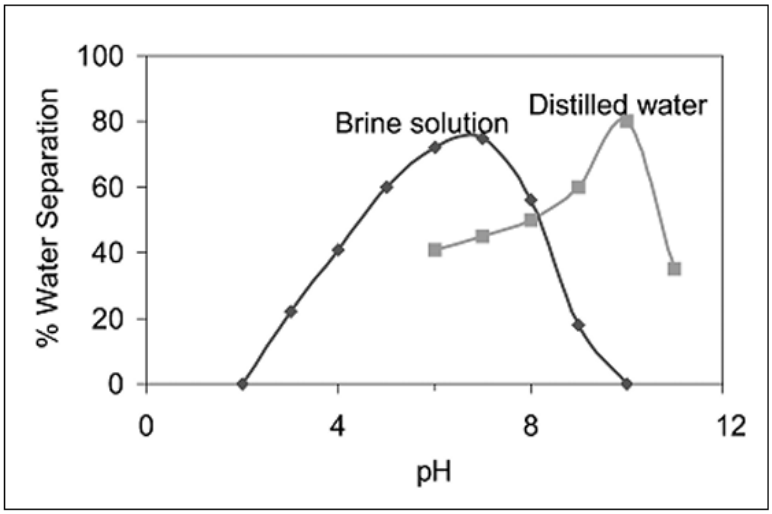

Figure II-5-b: Effect of brine and pH on emulsion stability [43]

The industry standard for measuring the acid content of crude oils is the Total Acid Number (TAN), which is defined by Equation (II.6) below.

$$TAN = \frac{mg\ KOH}{g\ Crude} \tag{II.6}$$

Crude oils with a Total Acid Number (TAN) greater than 1.0 are classified as high TAN crudes. Similarly, the Total Base Number (TBN) is defined as the amount of perchloric acid required to neutralize all the bases present in the crude.

II-5 Comparison between desalting technologies

This study examines the desalter design technologies offered by Cameron and NATCO, each utilizing a distinct approach to the desalting process. Cameron Petreco employs dielectric desalter technology, while NATCO utilizes Dual Polarity technology. Both technologies have their own advantages and specific operational considerations. Below are the key characteristics of each.

II-5-1 Cameron's Dielectric Technology

The Dielectric design [44] utilizes alternating current to polarize water molecules, facilitating the coalescence of water droplets. As shown in Figure II-6, Cameron's dielectric desalter features a three-grid electrode system and a horizontal emulsion distribution, ensuring efficient oil/water separation. This technology has demonstrated long-term reliability in refinery applications. Given that the existing desalter already employs dielectric technology, adopting the same approach for the second-stage desalter could offer operational advantages.

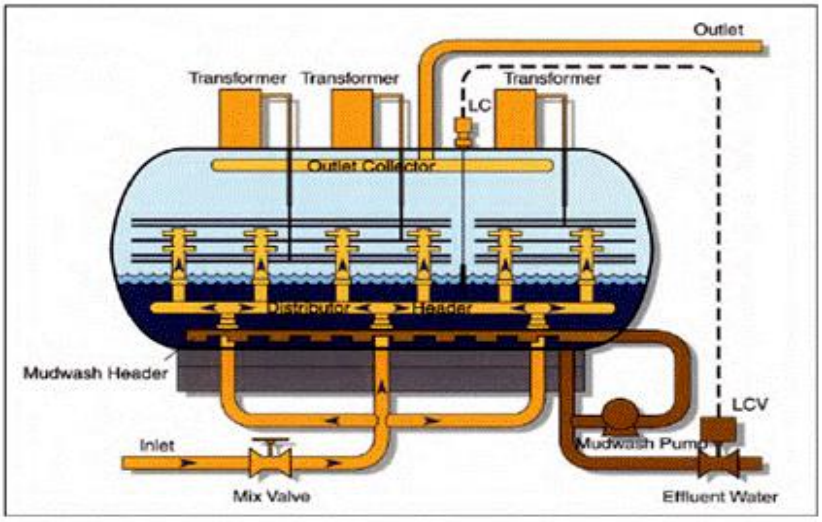

Figure II-6: Cameron dielectric® Dehydrator/Desalter [44]

II-5-2 NATCO's Dual Polarity Technology

Unlike the traditional AC current system, Dual Polarity technology [42] integrates both AC and DC fields for enhanced desalting efficiency. As the crude oil emulsion enters the system, it flows upward through the AC field, where free water immediately separates and settles in the water section of the vessel. Larger water droplets coalesce and separate due to the AC field, while smaller droplets remain suspended in the oil as it moves into the DC section. Within this section, the DC electrostatic field causes the remaining water droplets to coalesce and settle at the bottom of the vessel.

Utilizing the same reliable AC power supply as conventional electrostatic desalters, Dual Polarity technology employs rectifiers to split the high voltage into positive and negative components. Opposing electrode plates are charged accordingly, causing water droplets to elongate and be drawn toward a plate, acquiring its charge in the process.

This dual polarity electrostatic approach enables more thorough dehydration [45], allowing the system to process crude oil with higher viscosity. As a result, less heat is required to reduce oil viscosity under processing conditions. Figure II-7and II-8 illustrates NATCO's performance comparison between desalters using only AC fields versus those incorporating both AC and DC fields.

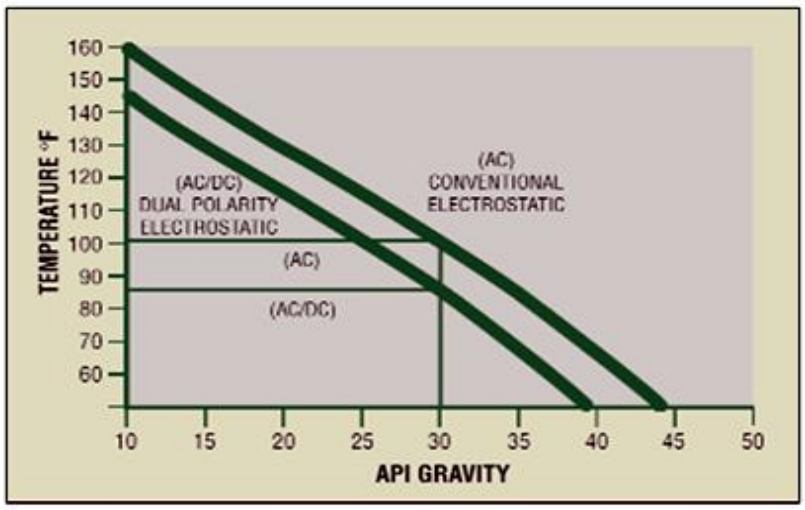

Figure II-7: Temperature requirement vs. API gravity [45]

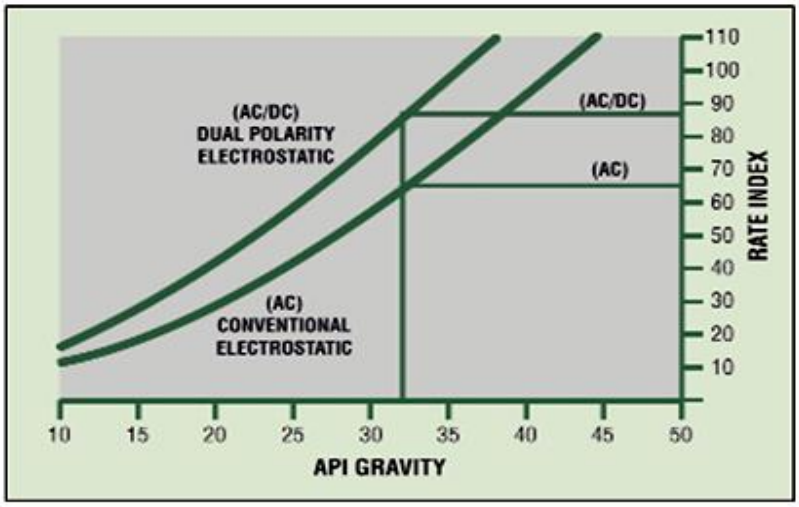

Figure II-8: Throughput vs. API gravity [45]

According to NATCO, the Dual Polarity electrostatic desalter requires less space because it can handle significantly higher flow rates compared to conventional desalters. The AC/DC process generates larger droplets than traditional AC units, allowing them to settle more easily through the opposing emulsion flow. As a result, a greater volume of oil can be processed within a vessel of the same size.

II-6 Electrical system for desalters

As previously mentioned, two desalter vendors, Cameron and NATCO, have been consulted to provide desalter technology for the revamp of the crude distillation unit. Each vendor employs different technologies to achieve the required desalting efficiency. A brief overview of each vendor's electrical system is outlined below.

II-6-1 Cameron's dielectric system

As previously explained, the dielectric system utilizes AC field technology for the removal of particulates. In an AC field, the rapid reversal of current prevents the formation and accumulation of corrosion products by reversing the chemical reaction before they can diffuse away from the reaction site. As a result, no net corrosion occurs.

The dielectric design utilizes a three-grid electrode system and horizontal emulsion distribution [44]. The basic configuration of this process is shown in Figure II-9.

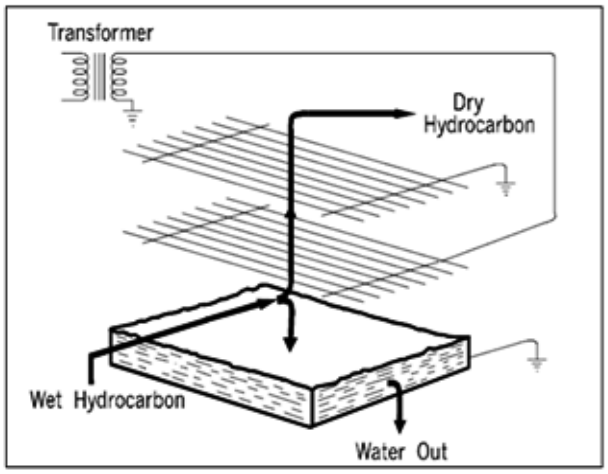

Figure II-9: AC Electrostatic coalescer [44]

According to Cameron, the electrical components of the dielectric system will include three 100 KVA, 60 Hz, single-phase power units (transformers), a level indicator, a switchboard panel equipped with three AC voltmeters/ammeters, a start/stop pushbutton housed in an explosion-proof enclosure, three voltage/current transmitters (4-20 mA) in explosion-proof housing, and a junction box for customer interface. Like most conventional electrostatic oil dehydration systems, the dielectric system utilizes reactance transformers to safeguard the electrical power supply. An internal reactor generates a voltage drop in series with the transformer's primary winding, thereby limiting power to the transformer windings. The total demand load for Cameron's dielectric system is 300 KVA, with an expected load of 60 KW for the second-stage desalter.

II-6-2 NATCO's dual polarity system

NATCO's dual polarity system employs a combination of AC and DC fields to leverage the advantages of both while mitigating the corrosion issues typically associated with a purely DC field. The basic configuration of this process is illustrated in Figure II-10.

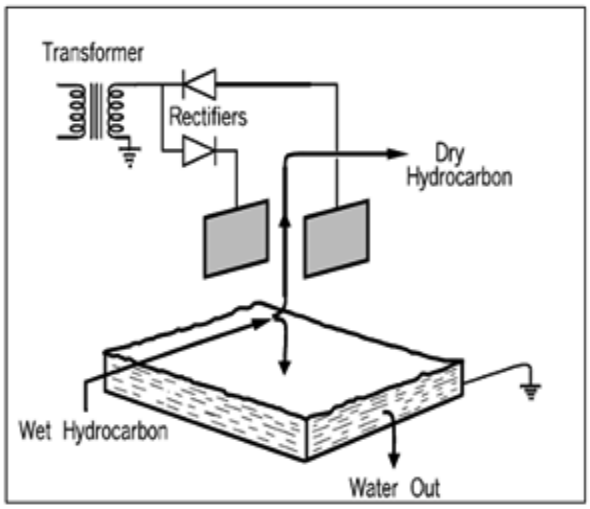

Figure II-10: Dual polarity AC/DC field [45]

The Dual Polarity system utilizes rectifiers to split high voltage into positive and negative components. Pairs of electrode plates are charged oppositely, causing water droplets entering the field to elongate and be drawn toward one of the plates, acquiring the charge of the approaching electrode.

According to NATCO, the electrical components of the Dual Polarity system will include one 100 KVA, 60 Hz, single-phase transformer with a built-in firing board SCR and rectifiers, a circuit breaker, level switches, primary circuit voltmeters, and PC-Load Responsive Controllers (PC-LRC). The built-in firing board SCR and PC-LRC are optional features that, according to the vendor, enhance tuning capabilities of power supply properties and provide higher tolerance for conductive crude [45].

Like most conventional electrostatic oil dehydration systems, the Dual Polarity system employs a reactance transformer to protect the electrical power supply. An internal reactor generates a voltage drop in series with the primary winding of the transformer, thereby limiting power to the transformer windings. The total demand load for the Dual Polarity system is 100 KVA, with an expected load typically around 30 % of the demand load [45].

II-7 Interface Level Control

The second key control function of a desalter is interface level control. The increasing trend of processing heavy crudes can result in thicker rag layers within the desalter, making it more challenging to maintain and control the interface level effectively.

Measurement of the water/oil interface position has commonly been attempted with analog type capacitance level transmitters [46]. However, the measuring probe of this type of

device may become covered with carbon, water emulsions, and other substances. This accumulation leads to interface position errors and ultimately makes the output signal unreliable. As shown in Figure II-11, the probe is unable to measure oil in a water-continuous mixture, and a high water cut near the top of the tank causes capacitance probes to display a full-scale reading.

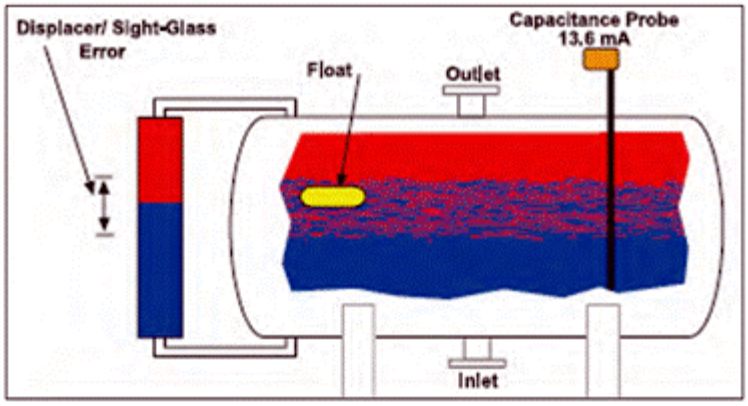

Figure II-11: Level control in the desalter using capacitance probe [46]

Another, more advanced method for level control is AGAR Interface Control. An improved control system not only enhances the efficient operation of the equipment but also helps prevent oil carryover into the brine system, which is directed to effluent treatment. Figure II-12 illustrates a typical AGAR level control system.

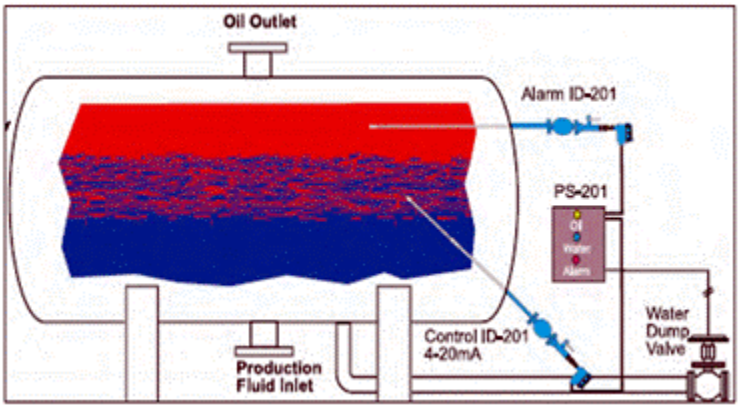

Figure II-12: Level control in the desalter using AGAR system [46]

The AGAR Concentration Control provides a current output proportional to the water content across the full scale of 0-100 %. This informs operators about the thickness of the emulsion pad and the direction in which the rag layer is expanding. Additionally, it allows operators to precisely control the level in the desired direction.

Chapter III

Practical Application: Monitoring and Calculation of Desalting Efficiency

Practical Application: Monitoring and Calculation of Desalting Efficiency

III-1 Introduction

This chapter will present all the physicochemical analyses of oil and water. We will also address the various calculations related to viscosity, density, salt content, and water-oil two-phase flow rates. Then, we will present the calculation results obtained for the desalting system, highlighting its efficiency, flow velocity, settling time, and residence time. Finally, a study was conducted for the simulation and optimization of the characteristics of the analyzed desalter.

III-2 Determination of Water-Oil Two-Phase Flow Rates

Daily measurement data from the desalting unit at UTBS were used to calculate the water-oil two-phase flow rates. Table (III.1) presents the results of the average values obtained from these measurements.

Table III.1: Results of the average measurements of water-oil flow rates

Measurement points	Desalter inlet (1) **Q_c (m^3/h)**	Desalter inlet (1) **Q_w (m^3/h)**	Desalter inlet (2) **Q_d (m^3/h)**	Desalter outlet (1) **$Q_{w'}$ (m^3/h)**	Wash water rate **Y (%)**
Average	480	2.88	466.0660	16.814	0.6

Considering that:

Q_c: Crude oil flow rate to be desalted.

Q_w: Wash water flow rate at the inlet such that $Q_w = Q_c \times Y$

Q_d: Desalted oil flow rate at the inlet such that $Q_d = \frac{Q_c \times (1-X)}{(1-Z)}$

$Q_{w'}$: Drain water flow rate $Q_{w'} = (Q_c + Q_w) - Q_d$

Y: The quantity of water injected relative to the crude oil, measured in (% vol) ($Y = 0.6\ \%$)

X: Water cut in the crude oil at the inlet of the desalter (%) ($X = 3\ \%$)

Z: Water content of the crude oil at the outlet of the desalter (%) ($Z = 0.1\ \%$)

Additional parameters to take into account when calculating the desalting capacity (material balance) includes the purge water flow rate ($Q_{w'}$) and the flow rate of desalted crude oil (Q_d). The total flow rate, denoted as (Q_T), is given by the following formula (III.1):

$$Q_T = Q_c + Q_w \quad \text{(III.1)}$$

$$Q_c + Q_w = Q_d + Q_{w'} \quad \text{(III.2)}$$

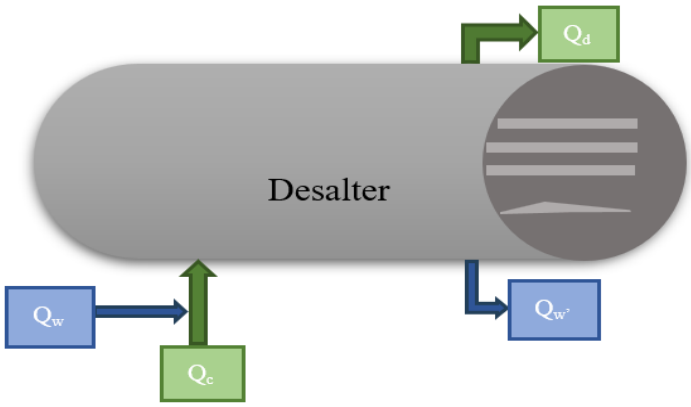

Figure III-1: Material balance schematic

The results of the flow rates, obtained after performing the material balance assessment of the desalting unit, are shown in Table (III.2) below.

Table III.2: Flow Rate Results from the Material Balance of the Desalting Unit

Flow rates (m^3/h)	Q_c	Q_w	Q_d	$Q_{w'}$
Results	480	2.88	466.0660	16.814

The quantity of desalted crude oil is calculated using formulas (III.3) below:

$$Q_d = \frac{Q_c \times (1-X)}{(1-Z)} \qquad \text{(III.3)}$$

$$Q_d = \frac{480 \times (1 - 0.03)}{(1 - 0.001)} = 466.0660$$

We find: $$\boldsymbol{Q_d = 466.0660\, m^3/h}$$

The quantity of purge water is calculated using the formula (III.4) below:

$$Q_{w'} = (Q_c + Q_w) - Q_d \qquad \text{(III.4)}$$

$$Q_{w'} = (480 + 2.88) - 466.0660$$

$$\boldsymbol{Q_{w'} = 16.814\, m^3/h}$$

III-3 Determination of process efficiency

The efficiency of the desalting unit is calculated by determining and monitoring the average salinity, which is based on the salinity levels at the inlet and outlet of the defaulters and is expressed as a percentage (Equation III.5).

$$E_{ff} = \frac{S_i - S_o}{S_i} \times 100 \qquad \text{(III.5)}$$

The results obtained after performing the calculations are presented in Table (III.3) below.

Table III.3: Process Efficiency Results of the Two Desalters

Desalter (1)			Desalter (2)		
Salinity (mg/l)		Efficiency (%)	Salinity (mg/l)		Efficiency (%)
Inlet (S_i)	Outlet (S_o)		Inlet (S_i)	Outlet (S_o)	
380	70	81.5789	70	22	68.5714

According to the efficiency values of the desalters, it was observed that the majority of the salts are removed in the desalter (1), while the remaining salts are removed in desalter (2), as the load at the inlet of desalter (1) is saltier than that of desalter (2).

III-4 Calculation results of the settling velocity

The analysis of settling velocity often involves the application of fluid dynamics principles. It takes into account various factors such as the size of water droplets, the density of solid particles, the viscosity of the fluid, and the geometric characteristics of the desalting system.

The study of the settling velocity of water droplets in the desalter helps determine the time required for the droplets to effectively separate from other components. This directly affects the efficiency of the desalting process, as well as the design of the equipment, particularly settlers or centrifuges used in desalting facilities.

The determination of settling velocity was carried out by applying Stokes' Law (Equation III.6)

According to the STOKES Formula.

$$V_d = \left[\frac{4}{3}.\frac{(d_d - d_c)}{d_c}.\frac{D.g}{\Phi}\right]^{\frac{1}{2}} \quad \text{(III.6)}$$

Or:

V_d: settling velocity (m/s).

d_d: density of the dispersed phase.

d_c: density of the continuous phase.

D: diameter of water droplets.

g: acceleration due to gravity.

Φ: friction coefficient that depends on the flow regime.

a) Determination of the friction coefficient

We determine the friction coefficient (Φ) as a function of the Reynolds number.

$$Re = \frac{V_d.D}{\vartheta} \quad \text{(III.7)}$$

Where:

V_d: flow velocity.

D: droplet diameter.

ϑ: fluid viscosity.

We assume that the flow regime in the desalination unit is laminar, we determine the resistance coefficient $\Phi = f(R_e)$ then, we checks if the assumed regime is correct.

Table III.4: The flow regime and the friction coefficient

Flow regime	**R_e**	**Φ**
Laminar	$R_e \leq 0.2$	$24/R_e$
Transitory	$0.2 < R_e < 500$	$18.5/R_e^{0.6}$
Turbulent	$R_e \geq 500$	$44/R_e$

Since we assumed that the flow regime is laminar, therefore $\Phi = 24/Re$

The STOKES relation (III.8) becomes:

$$V_d = \left[\frac{1}{18}.g\,\frac{(d_d - d_c)}{d_c}\frac{D^2}{\vartheta_c}\right] \quad \text{(III.8)}$$

b) Determination of the water droplet diameter

According to table III.5, we plot figure III-2 to determine the droplet diameter of water.

Table III.5: Determination of water droplet diameter

water content + washing rate	1	2	3	4	5
Diameter of the droplet (10^{-5} m)	6	7.5	9	13	17

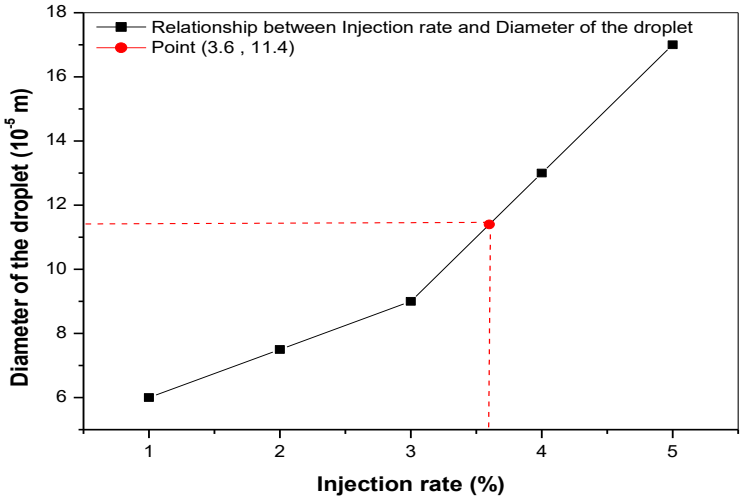

Figure III-2: variation of the water droplet as a function of water content and washing rate

In our case, the wash rate plus the water content is 3.6 % (Y+X = 3.6 %), and for the droplet diameter, we have (D = 11.4×10^{-5} m). The calculation of the settling velocity is initiated using the following method:

a) A flow regime is provisionally proposed.
b) The corresponding settling velocity is calculated.
c) It is verified whether the proposed flow regime matches the actual flow regime.

In the first case, it is proposed that the flow regime is turbulent. To do this, the viscosity of crude oil at 70 °C needs to be determined; however, this value is not available in the laboratory. Therefore, the viscosities at 20 °C and 38 °C are used instead, corresponding to 2.45 and 1.79 cSt, respectively.

Subsequently, applying the Gross equation (Equation III.9) where the **GROSS** relation is used:

$$\text{Log}\ \frac{\vartheta_{t1}}{\vartheta_{t2}} = \text{R}.\text{Log}\ \frac{t_2}{t_1} \qquad \text{(III.9)}$$

The coefficient R is determined first: $\text{R} = \dfrac{\text{Log}\ \frac{\vartheta_{t1}}{\vartheta_{t2}}}{\text{Log}\ \frac{t_2}{t_1}}$

By numerical application, we find:

$$\text{R} = \frac{\text{Log}\ \frac{2.45}{1.79}}{\text{Log}\ \frac{38}{20}}$$

$$\mathbf{R = 0.4890}$$

Subsequently, the viscosity at the desalting temperature (70 °C) is determined using Equation (III.9):

$$\text{Log}\,\vartheta_{t2} = \text{Log}\,\vartheta_{t1} - \text{R.}\,\text{Log}\,\frac{t_2}{t_1}$$

By numerical application, we find:

$$Log\,\vartheta_{70} = Log\,2.45 - 0.4890.\,Log\,\frac{70}{20}$$

$$\boldsymbol{\vartheta_{70} = 1.3277\ cSt}$$

Furthermore, the density corresponding to the temperature of 70 °C is calculated.

1- The density at 15 °C is determined through the physicochemical analysis of crude oil: $d_{15°C} = 0.8040$

2- The density at the desalting temperature is then determined by applying the following formula (Equation III.10):

$$d_{t2} = d_{t1} - \alpha(t_2 - t_1) \qquad \text{(III.10)}$$

Where:

d_{t2}: Density at the given temperature.

d_{t1}: Density at the initial temperature.

α: Coefficient that characterizes the variation of density as a function of temperature, with:

$$\alpha = 0.001828 - 0.00132\,(d_{t1})$$

t_2: Given temperature.

t_1: Initial temperature.

In our case, we find: $d_{20} = d_{15} - \alpha(20 - 15)$

By numerical application, we obtain the following results:

$$\alpha = 0.001828 - 0.00132\,(d_{15}) = 0.001828 - 0.00132\,(0.8040)$$

$$\boldsymbol{\alpha = 0.00076672}$$

The density is then calculated accordingly:

$$d_{20} = 0.8040 - 0.00076672\,(20 - 15)$$

$$\boldsymbol{d_{20} = 0.8001}$$

The density at the desalting temperature is:

$$d_{70} = d_{20} - \alpha(70 - 20)$$

By numerical application, we obtain the following results:

$$\alpha = 0.001828 - 0.00132\,(d_{20}) = 0.001828 - 0.00132\,(0.8001)$$

$$\boldsymbol{\alpha = 0.00077186}$$

The density is then calculated accordingly:

$$d_{70} = 0.8001 - 0.00077186\,(70 - 20)$$

$$\mathbf{d_{70} = 0.7615}$$

Therefore, the density of water is:

$$\mathbf{d_{70} = 0.9624}$$

All the results are summarized in Table (III.6) below:

Table III.6: Calculation of Crude Oil Viscosity and the Density of the Oil and Water Phases

Parameter	Viscosity (cSt)	Density of the oil	Density of water
Desalting temperature (70 °C)	1.3277	0.7615	0.9624

In this case, it is proposed that the flow regime is laminar; therefore, Stocks equation (Equation III.8) is applied.

$$V_d = \left[\frac{1}{18}.g\,\frac{(d_d - d_c)}{d_c}\frac{D^2}{\vartheta_c}\right]$$

$$V_d = \left[\frac{1}{18} \times 9.81 \times \frac{(962.4 - 761.5)}{761.5}\frac{(11.4 \times 10^{-5})^2}{1.3277 \times 10^{-6}}\right]$$

Therefore: $$\mathbf{V_d = 1.4073 \times 10^{-3}\ m/s}$$

We will verify the flow regime by calculating the Reynolds number using equation (III.7):

By numerical application, we find: $\mathrm{Re} = \frac{1.4073\times10^{-3}\times11.4\times10^{-5}}{1.3277\times10^{-6}}$

$$\mathbf{Re = 0.1208}$$

$\mathbf{R_e}$ is less than 0.2, so the flow regime is laminar.

III-5 Settling Time Calculation Results

The settling time is given by the following formula (III.11):

$$T_d = \frac{L_1}{V_d} \qquad \text{(III.11)}$$

Where:

T_d: Settling time (min).

L_1: Distance between the lower electrode and the interface (L_1 = 0.2 m).

V_d: Settling velocity (m/s).

$$T_d = \frac{0.2}{1.4073 \times 10^{-3}}$$

Therefore: $\mathbf{T_d = 2.3686\ min}$

III-6 Residence Time Calculation Results

The residence time is determined by the following equation (III.12):

$$T_s = \frac{V}{Q_T} \quad \text{(III.12)}$$

Where:

T_s: residence time (min).

V: volume of the desalter (m^3).

Q_T: volumetric flow rate of the feed (m^3/h).

$$Q_T = Q_c + Q_w$$

$$Q_T = 480 + 2.88$$

$$\boldsymbol{Q_T = 482.88\ m^3/h}$$

Thus, the volume of the desalter is calculated using equation (III.13):

$$V = V_1 + V_2 \quad \text{(III.13)}$$

Where:

V: volume of the desalter (m^3).

V_1: volume of the cylindrical part of the desalter (m^3).

V_2: volume of the two hemispheres (m^3).

Hence:

$$V = \pi\frac{D^2}{4}L + \frac{4}{3}\pi\frac{D^3}{8} \quad \text{(III.14)}$$

$$V = \pi\frac{3^2}{4}12 + \frac{4}{3}\pi\frac{3^3}{8}$$

$$\mathbf{V = 98.9601\ m^3}$$

Finally, the residence time is determined: $T_s = 98.9601/482.88$

$$\mathbf{T_s = 12.294\ min}$$

In order to prevent separated water from being carried along with the desalted crude oil, the settling time should be **shorter than** the residence time.

III-7 Sizing of the Desalter

III-7-1 Electrical Properties

The electrical properties of the desalter allow us to assess its performance. For the desalter to function properly, it is necessary that the electric field (E) between the electrodes be lower than the critical field (EC).

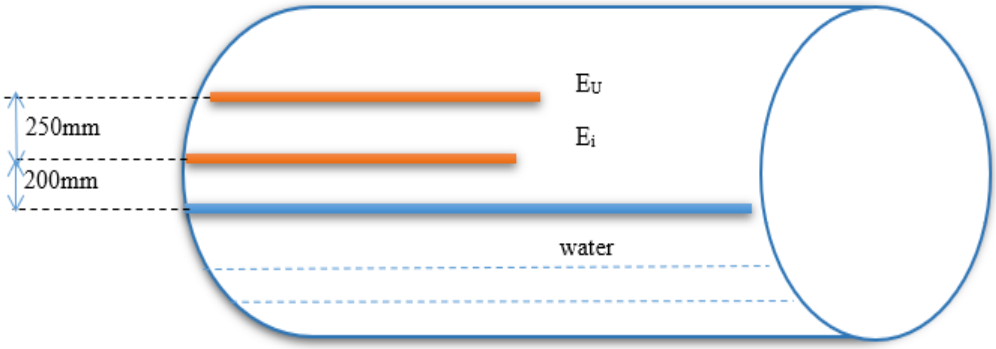

Figure III-3: Representation of the distance between the electrode and the water phase

The electric field between two electrodes is calculated using the following formula (III.15):

$$E = U/L \quad \text{(III.15)}$$

With:

E: electric field between the electrodes (V/cm).

U: voltage of the current (20000 V).

L: distance between the electrodes (25 cm).

Therefore:

$$E = 20000/25$$

$$\mathbf{E = 800\ V/cm}$$

The electric field between the high water level and the lower electrode is calculated using the following formula (III.16):

$$E_1 = U/L_1 \quad \text{(III.16)}$$

Where:

E_1: electric field between the high water level (interface) and the lower electrode (V/cm).

U: voltage of the current (20000 V).

L_1: distance between the high water level and the lower electrode (20 cm).

$$E_1 = 20000/20$$

$$E_1 = \mathbf{1000\ V/cm}$$

For the proper functioning of the desalter, the electric field (E) between the electrodes must be lower than the critical field (E_c) $\{\mathbf{E < E_c}\}$.

The critical electric field is calculated using Equation (III.17):

$$E_c = A'\sqrt{\frac{2.\delta}{\varepsilon.D}} \qquad \text{(III.17)}$$

- **Determination of the proportionality coefficient**

According to table, we plot the curve A' = f (y + x) (figure III-4) and derive the value of the proportionality coefficient (A').

Table III.7: Proportionality coefficient (A') as a function of water content plus washing rate (Y+X).

(Y+X) %	01	05	10	20
A'	376	382	391	403

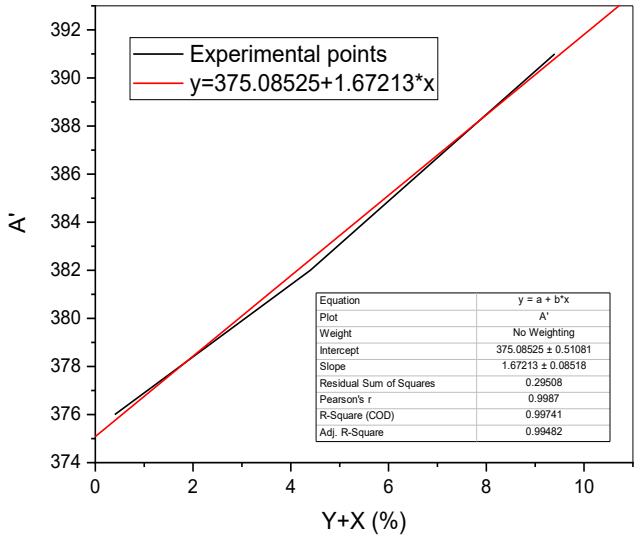

Figure III-4: variation of the proportionality coefficient (A') as a function of the washing rate

Where:

δ: Interfacial tension between water and oil (15 g/cm²).

ε: Dielectric constant =16.

D: Diameter of the water droplet (11.4×10^{-3} cm).

A': Proportionality coefficient (for a wash rate of 3.6 %, A' = 381.1049)

Therefore:
$$E_c = 381.1049 \times \sqrt{\frac{2\times15}{16\times11.4\times10^{-3}}}$$

$$\mathbf{E_c = 4887.5672\, V/cm}$$

According to the results obtained, it is observed that the electric field (E) between the electrodes is lower than the critical electric field, which confirms the proper functioning of the desalter under study.

III-7-2 Theoretical and Actual Efficiency of the Desalting System

The parameters that influence the optimal performance of the desalter are the efficiency of the desalter itself and that of the desalting process (theoretical estimation). These can be expressed in terms of the various parameters involved in the desalting process (Equation III.18).

$$A = \frac{Z\times\left(S_i + \frac{Y\times S_w}{100}\right)}{X+Y} \qquad \text{(III.18)}$$

With:

A: Theoretical optimal salt concentration in the crude oil at the outlet of the desalter, measured in (mg/l).

S_i: Salt concentration in the oil phase at the inlet of the desalter, measured in (mg/l).

S_w: Salt concentration in water dilution (wash water), measured in (mg/l).

X: Water cut in the crude oil at the inlet of the desalter (%).

Y: Amount of water injected (wash water) relative to the crude oil, measured in (% vol).

Z: Water content of crude oil at the outlet of the desalter (%).

The numerical calculation begins using the following initial data:

S_i =380 mg/l

S_w = 1945mg/l

X = 3%

Y = 0.6%

Z =0.1%

$$A = \frac{0.1 \times \left(380 + \frac{0.6 \times 1945}{100}\right)}{0.6 + 3}$$

$$\mathbf{A = 10.8797\ mg/l}$$

On the other hand, the efficiency of the desalter is given by the formula (III.19) below:

$$E_{ffT} = \frac{(S_i - S_o)}{S_i} \times 100 \qquad \text{(III.19)}$$

Where:

E_{ffT}: Actual efficiency of the desalting system

S_i: Salt content of the crude oil at the inlet of the desalter

S_o: Salt content of the crude oil at the outlet of the desalter

$$E_{ffT} = \frac{(380 - 22)}{380} \times 100$$

$$\mathbf{E_{ffT} = 94.2105\ \%}$$

Formula (III.20) gives the expression for the theoretical efficiency of the desalting process:

$$E_{Th} = \frac{(S_i - S_o)}{S_i - A} \times 100 \qquad \text{(III.20)}$$

$$E_{Th} = \frac{(380 - 22)}{380 - 10.8797} \times 100$$

$$\mathbf{E_{Th} = 96.9873\ \%}$$

III-7-3- Calculation of the distributor

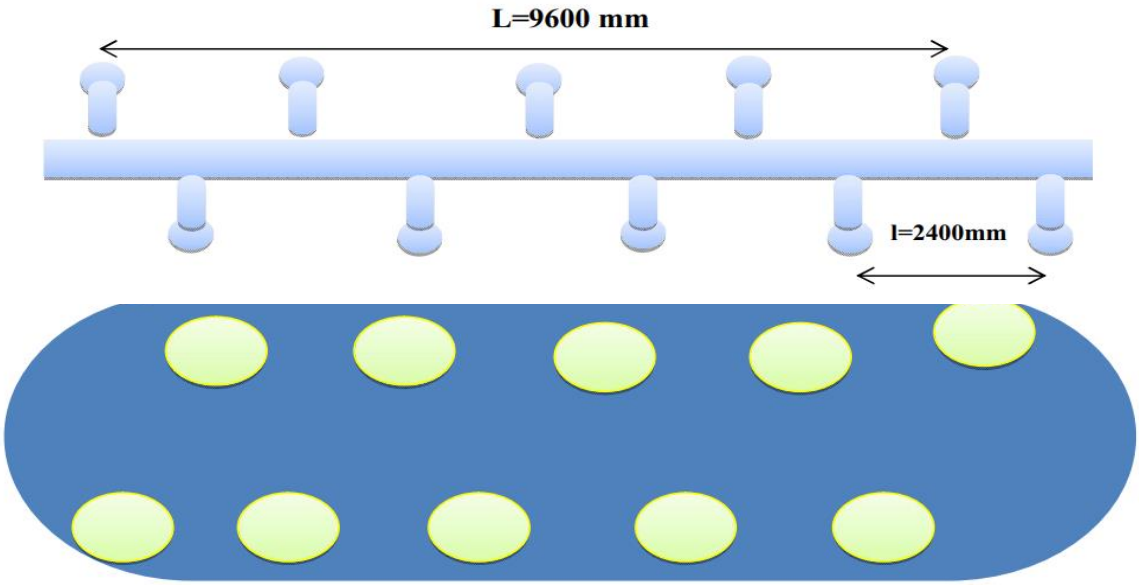

Figure III-5: Representation of the distributor

The purpose of the distribution calculation is to determine the settling velocity and the permissible velocity of the crude oil through the distributor holes. Increasing the velocity improves the distribution of oil along the length of the desalter; however, high velocities can lead to strong turbulence in the emulsion.

For the calculation of the distributor, the following steps must be followed:

a) Calculation of the number of distribution ramps

The number of distribution ramps is given by the following formula (III.21):

$$n = \frac{L}{l} + 1 \qquad \text{(III.21)}$$

L: Distance between the two outermost holes (L = 9600 mm)

l: Distance between the two ramps (l = 2400 mm)

(+1): Corresponds to the two halves of the end holes

Therefore, according to formula (III.21), we proceed with the numerical application.

$$n = \frac{9600}{2400} + 1$$

$$\mathbf{n = 5\ ramps}$$

In each distribution ramp, there are 2 holes. Therefore, the total number of holes will be equal to 10.

b) Calculation of Flow Velocity

Crude oil has a flow velocity that can be calculated using the following formula (III.22):

$$W = \frac{Q_c}{3600.2n.f} \qquad \text{(III.22)}$$

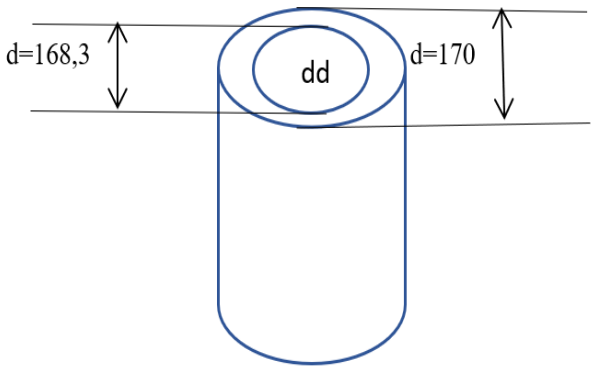

Figure III-6: Representative schematic of distributor hole dimensions

According to the diagram, the cross-sectional area of a single hole (f) is calculated as follows:

$$f = \frac{\pi}{4}.d^2 \quad \text{(III.23)}$$

Where:

W: Flow velocity (m/s)

Q_c: Flow rate of the feed (Q_c = 480 m³/h)

n: Number of distribution ramps

f: Cross-sectional area of a single hole (m²)

d: Inner diameter of a hole (d = 168.3 mm)

$$f = \frac{\pi}{4} \times (0.1683)^2$$

$$\mathbf{f = 22.2463 \times 10^{-3} m^2}$$

$$W = \frac{480}{3600 \times 10 \times 22.2463 \times 10^{-3}}$$

$$\mathbf{W = 0.5993\ m/s}$$

III-8 Modeling and simulation

III-8-1 Modeling using Population Balance Equation (PBE)

This section describes in detail the development and realization of the MATLAB script (**DESALTING_UTBS_Complete_Optim.m)**, designed to model and optimize a crude oil desalting unit. The objectives are twofold:

(i) Extract mathematical model parameters from experimental data (salinity vs. wash water fraction, demulsifier flow rate, and temperature) (**Tables S_1-S_3,** Supplementary Material).

(ii) Perform a global optimization of operating variables to achieve 99 % desalting efficiency (E) under salinity constraints using a Population Balance Equation (PBE) [47, 48] solved by Differential Evolution (DE) [49-51].

By following a structured workflow-data preprocessing, parameter fitting, visualization, and stochastic optimization-this script combines empirical adjustment with advanced met heuristic search to identify optimal operating conditions.

III-8-1-1 Mathematical model

a- Exponential decay models

Empirical observations suggest that the residual salinity S after treatment decays exponentially with each control variable. We therefore posit three sub-models (Table III.8):

Table III.8: Sub-models for each operational factor on salt removal

Parameter Identification	**Exponential Decay Models**	**Initial salinity**
Wash-water fraction **X** (%)	$S(X) = S_i^{(X)}.e^{-K_1(X)}$ (III.24)	$S_i^{(X)} = 245\ mg/L$
Demulsifier flow rate **Qd**(L/h)	$S(Q_d) = S_i^{(Q_d)}.e^{-K_2(Q_d)}$ (III.25)	$S_i^{(Q_d)} = 249\ mg/L$
Temperature **T** (°C)	$S(T) = S_i^{(T)}.e^{-K_3(T-64)}$ (III.26)	$S_i^{(T)} = 261\ mg/L$

From each model, we compute desalting efficiency; $E_{ff} = \frac{S_i - S_o}{S_i} \times 100$ (Equation III.5).

b- Global performance model

To capture combined effects and recycling, we define the operational vector ($P = X, Q_d, T, X_{recycle}$) with bounds:

-Wash water fraction: X ϵ [0, 10] %.

-Demulsifier flow rate: Q_d ϵ [0.35, 5] L/h.

-Temperature: T ϵ [64, 80] °C.

-Recycle water fraction: $X_{recycle}$ ϵ [0, 100] %.

The global driving function *F(P)* is taken as a linear combination of the fitted decay coefficients:

$$F(P) = [K_1(X) + K_2(Q_d)] \times \left(1 + \frac{X_{recycle}}{100}\right) + K_3(T - 64) \quad \text{(III.27)}$$

The final efficiency follows the equation (III.28):

$$E(P) = \left(1 - e^{-F(P)}\right) \times 100 \quad \text{(III.28)}$$

The global optimization studied to achieve 99 % desalting efficiency, requires $\{F(P) = \ln(100) = 4.6052\}$, and in addition the global outlet salinity ($S_O^{(Global)}$) must satisfy the commercial constraint (≤ 40 mg/L), with a maximum global inlet salinity $\{S_i^{(Global)} = 1302\ \frac{mg}{L}\}$.

$$S_O^{(Global)} = S_i^{(Global)} \times e^{-F(P)} \quad \text{(III.29)}$$

We have translated the empirical desalting study into a fully functional MATLAB implementation:

Step 1: fits exponential decay constants (k_1, k_2, k_3) via the function {lsqcurvefit}.

Step 2: employs a custom Differential Evolution algorithm to satisfy a 99 % efficiency target under a salinity constraint.

This modular approach estimation followed by global optimization allows easy extension and provides a robust framework for industrial process tuning (See **Figure III-7**).

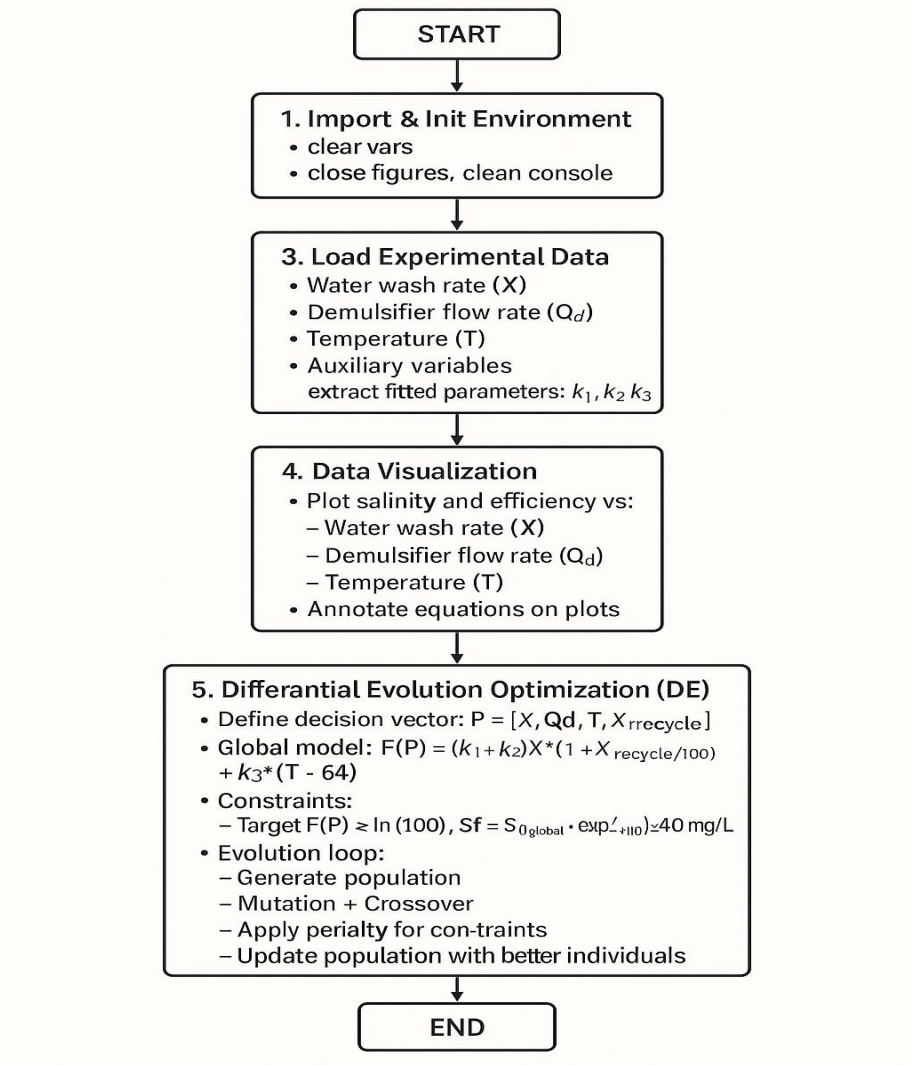

Figure III-7: The MATLAB script organigram used for global optimization (Our work)

c- Optimization results

The modeling work demonstrates how experimental data and a simplified PBE model can be combined with global search heuristics to optimize a complex industrial process. The MATLAB script serves as a blueprint for similar applications in chemical engineering, where exponential decay laws and evolutionary algorithms yield robust operational settings.

To reduce the final global outlet salinity ($S_O{}^{(Global)}$) of the desalting oil process; several parameters were studied such as: wash water fraction, chemical demulsifier flow rate, temperature control, and water recycling.

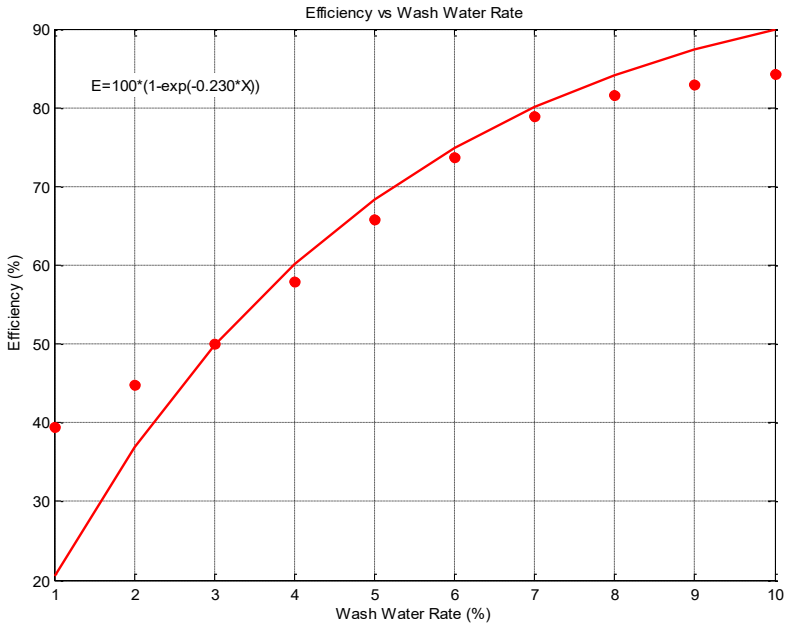

Figure III-8: Effect of wash water rate on efficiency.

The figure III-8 shows that efficiency increases with the wash water rate, following an exponential trend. This indicates that higher wash water rates improve the separation efficiency, but the rate of improvement decreases at higher levels, suggesting diminishing returns.

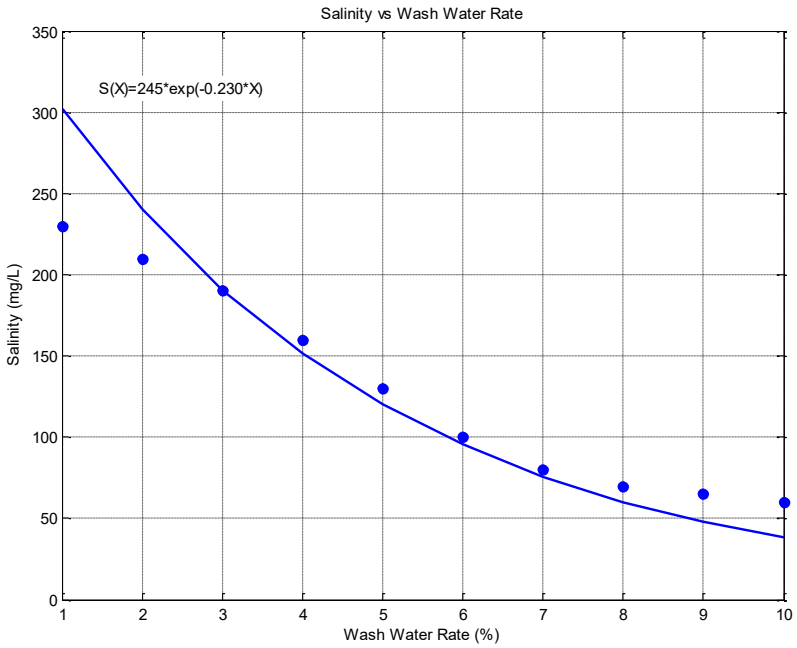

Figure III-9: Effect of wash water rate on salinity.

The graph shows that salinity decreases exponentially with increasing wash water rate. This indicates that higher amounts of wash water enhance the removal of salts, leading to improved desalting efficiency (See Figure III-9).

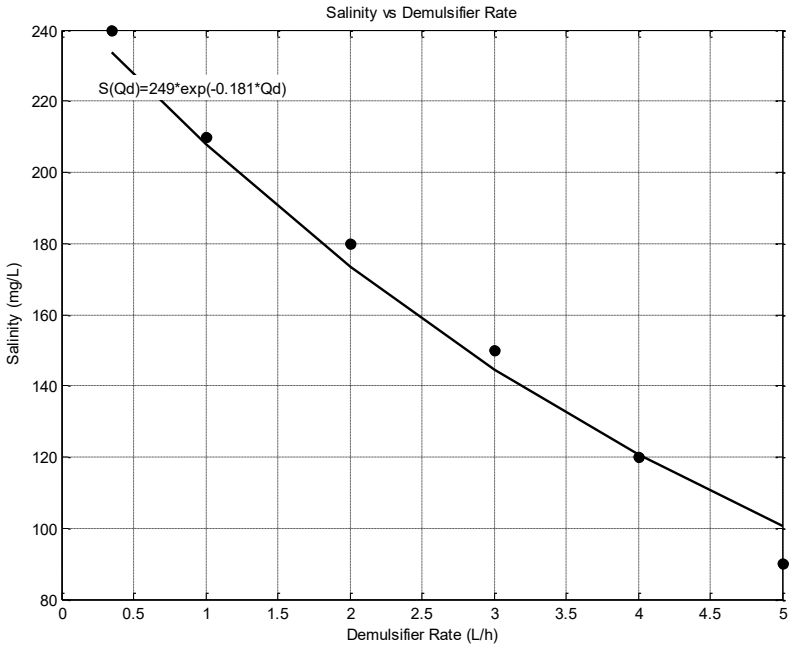

Figure III-10: Effect of demulsifier rate on salinity.

The graph (Figure III-10) demonstrates that salinity decreases with increasing demulsifier rate, following an exponential decay trend. This suggests that higher dosages of demulsifier enhance the separation process, effectively reducing the salt content.

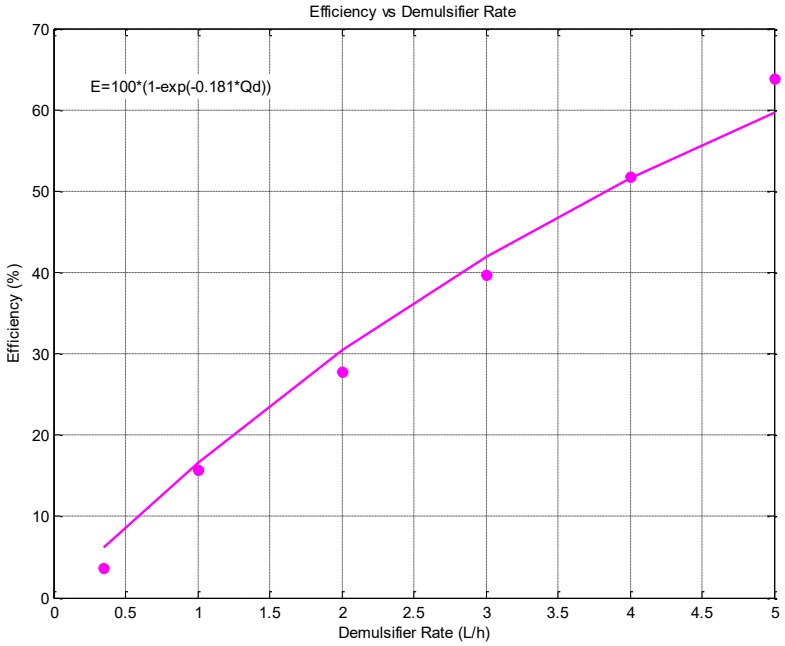

Figure III-11: Effect of demulsifier rate on efficiency.

The figure III-11 indicates that efficiency increases steadily with the demulsifier rate. This suggests a positive correlation between the amount of demulsifier used and the separation efficiency, with higher doses leading to improved performance.

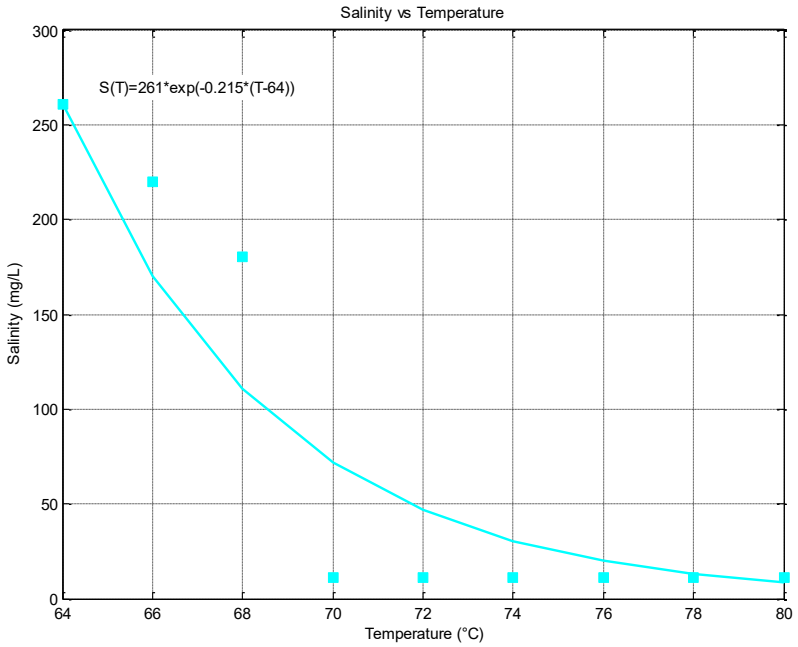

Figure III-12: Effect of temperature on salinity.

In figure III-12; the plot shows that salinity decreases exponentially with increasing temperature. This indicates that higher temperatures enhance the separation of salt from the mixture, leading to lower salinity levels at elevated temperatures.

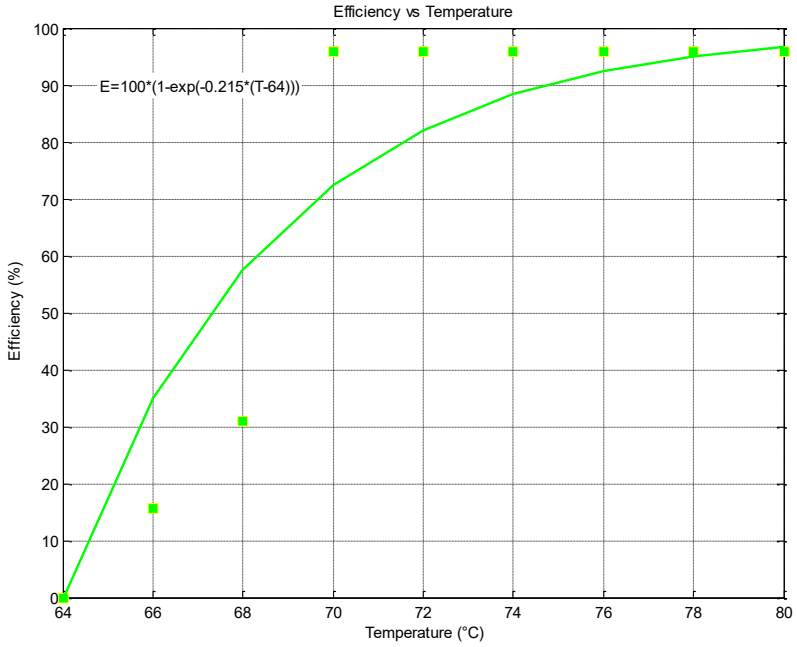

Figure III-13: Effect of temperature on efficiency.

The figure III-13 shows that efficiency increases rapidly with temperature at lower ranges, then gradually levels off as it approaches a maximum near 99 %. This suggests a diminishing return effect, where increasing temperature beyond a certain point yields only marginal improvements in efficiency.

The values of optimized parameters are presented in Table III.9.

Table III.9: Optimization results

Optimized washing water rate	X = 6.5591 %
Optimized demulsifier flow rate	Q_d = 1.4287 L/h
Optimized temperature	T = 70.7500 °C
Percentage of recycled water	$X_{recycle}$ = 16.9590 %
Achieved efficiency	E= 99.00 %
Final global outlet salinity	$S_o^{(Global)}$ =13.02 mg/L

III-8-2 Simulation of desalting unit using Aspen HYSYS

With the help of the Aspen HYSYS software (V.14), we are studying the temperature parameter to improve the process of removing salts found in crude oil. Desalting is an operation carried out to remove the salt contained in crude oil, as the latter presents several disadvantages at the level of installations (fouling, clogging, etc.). This elimination is linked to international standards for salt content in crude oil (≤ 40 mg/l).

In this section, we will simulate a desalination operation at the level of treatment unit (UTBS) in HASSI MESSAOUD (HMD) in parallel with obtaining the results for the actual possible variation at the desalination unit. The operational method we adopted was based on the reality of the desalination operation, where we will vary the temperature parameter and hold both (washing water, demulsifier) constant.

Engineers engaged in design engineering use Aspen HYSYS software to make fast calculations using efficient models and optimal techniques. For oil refining, gas processing and hydrocarbon applications, the most recommended thermodynamic model for simulation by Aspen HYSYS is the PENG-ROBINSON equation, as it correctly solves phase separation problems and makes it possible to predict liquid densities more in agreement with the actual values than the other equations.

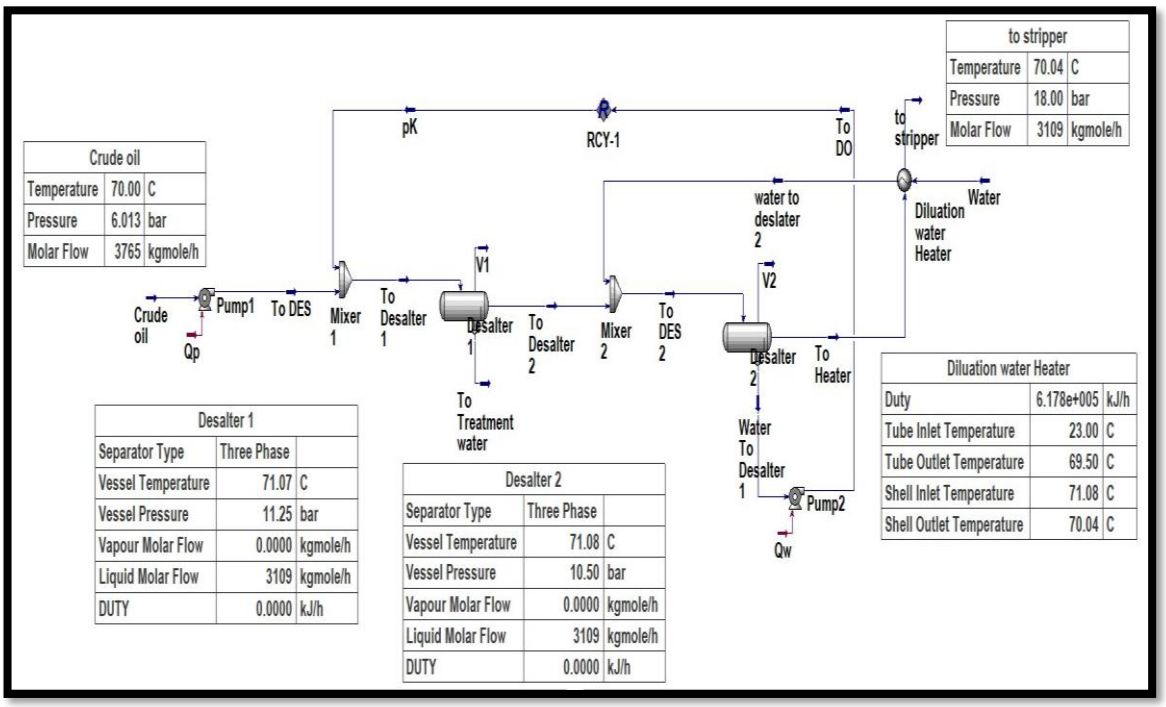

Figure III-14: Simulated Algerian crude oil desalting unit -Aspen HYSYS V14-

Table III.10: Effect of temperature changes on the process of desalting crude oil

T (°C)	64	65	66	67	68	69	70	71	72
Removed Salts (mg/L)	16.2	77.9	136.2	181.7	259.5	317.9	379.5	437.9	496.3
T (°C)	73	74	75	76	77	78	79	80	/
Removed Salts (mg/L)	541.7	600.1	554.7	733.1	775.3	833.7	888.9	947.2	/

Using the Aspen HYSYS software, we observe the effect of temperature on the desalination process, and this is what we notice in Figure III-14, a study of salt removal in crude oil at a temperature between 64 °C and 80 °C. We studied how temperature affects salt removal from crude oil using Aspen HYSYS software, and we found that the best temperature for removing salt is 70 °C, as we were able to reduce the salt concentration from 380 mg/L to 379.5 mg/L during our internship at the UTBS unit.

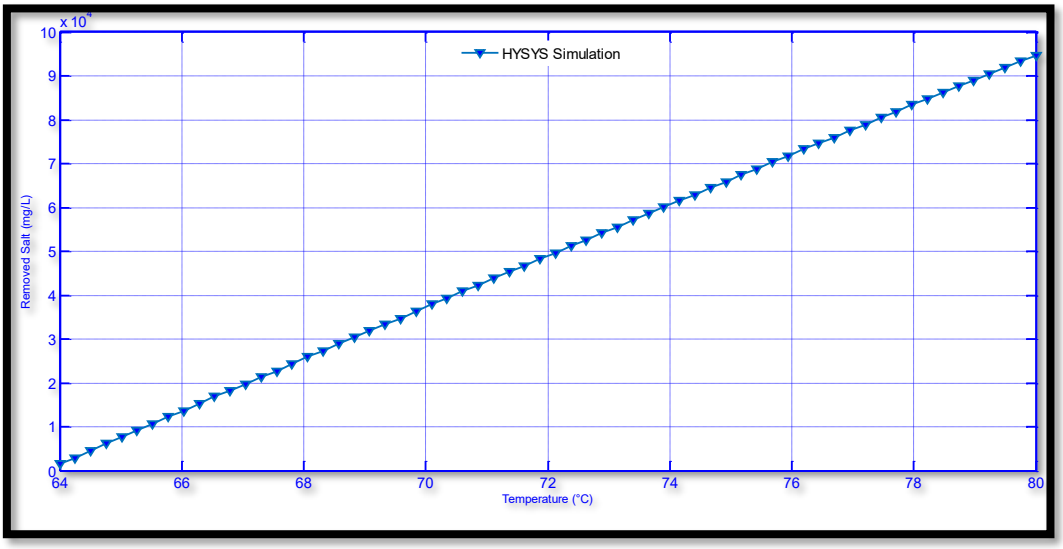

Figure III-15: Relationship between removed salts and Temperature

General conclusion

General conclusion

The work is part of a graduation project based on the field internship done at the UTBS unit located at Hassi Messaoud (HMD), Algeria. It deals with the function of the Desalting Unit for the treatment of crude oil to remove inorganic salts, mitigate corrosion and avoid deposits that could negatively impact the performance of downstream petroleum equipment.

This study has demonstrated a multi-level, comprehensive approach to optimizing crude oil desalting by linking field data analysis, basic fluid-dynamic calculations, population-balance modeling, global optimization algorithms, and process simulation. Daily material-balance measurements made on the UTBS unit provided actual inlet flow rates and salinity, outlet flow rates and salinity, which permitted a calculation of a desalting efficiency under operational conditions.

The basic analyses used Stokes' law to demonstrate droplet settling, Reynolds-number calculations to verify the flow regime, and residence-time calculations used for sizing the equipment, all supported an appropriate geometry and operating conditions for effective phase separation. Calculated electrical fields were below the critical value for coalescence with electrical current applied, proving the desalter unit stage was designed for stability.

Development of a Population Balance Equation (PBE) model based on experimental measurements of salinity versus wash-water, demulsifier and temperature enabled a prediction of salt-removal behavior. The PBE model was embedded in a Differential Evolution optimization routine in MATLAB, and the optimum operating conditions were found: wash-water fraction X = 6.56 %, demulsifier rate Q_d = 1.43 L/h, temperature T = 70.75 °C, and recycle fraction $X_{recycle}$ = 16.96 %. These conditions produced 99 % desalting efficiency while maintaining outlet salinity at 13.02 mg/L, which is well below the industrial limit of 40 mg/L.

The consistent HYSYS simulations further supported the temperature dependency of salt removal, providing evidence that a process temperature near 70 °C would yield the least residual salinity, similar to experimental outcomes. This co-validation with experimental optimization and methodical simulation supports the credibility of the approach towards industry. Overall, the methodologies presented in this manuscript provide an applicable framework for crude oil treatment units to optimize for better desalting performance. Future work may also utilize this approach for multi-objective optimization (for example, minimizing energy vs. maximizing efficiency), dynamic operational situations, and scaling up, expanding the applicability of this work across a diverse grade of crude oils and different plant configurations.

Bibliographic references

Bibliographic references

1. Wauquier, J. P. (1998). Le raffinage du pétrole brut: procédés de séparation (Vol. 2, pp. 240–260). Édition Technip.

2. Speight, J. G. (2014). The chemistry and technology of petroleum (5th ed.). CRC Press.

3. Ashrafizadeh, S. N., & Kamran, M. (2010). Emulsion breaking techniques in enhanced oil recovery: Chemical and electrostatic approaches. Journal of Petroleum Science and Engineering, 70(1–2), 99–110. https://doi.org/10.1016/j.petrol.2009.10.005

4. U.S. Energy Information Administration. (2022). What makes crude oil valuable – and why there are different types. https://www.eia.gov/todayinenergy/detail.php?id=26752

5. Hussein, A. (2023). Essentials of flow assurance solids in oil and gas operations. Gulf Professional Publishing.

6. Viswanathan, B. (2017). Energy sources. Elsevier.

7. Gary, J. H., Handwerk, G. E., & Kaiser, M. J. (2007). Petroleum refining: Technology and economics (5th ed.). CRC Press.

8. David, R. (2008). Handbook of chemistry and physics (89th ed., pp. 9–50). CRC Press.

9. TOTAL. (2007). Manuel de formation – Cours EXP-PR-EQ090 (pp. 4–97).

10. SONATRACH. (2010). Manuel opératoire de l'unité de traitement brut Hassi Messaoud Sud (UTBS).

11. Adams, F., Walstra, P., Brooks, B., Richmond, H., & Binks, B. (1998). Modern aspects of emulsion science. Royal Society of Chemistry.

12. Salager, J. L., & Anton, R. (2006). Formulation des émulsions par la méthode du HLD. Techniques de l'Ingénieur.

13. Tadros, T. F. (2013). Emulsion formation, stability, and rheology. In Emulsion formation and stability. Wiley-VCH Verlag GmbH & Co. KGaA.

14. Fuquan, T. (2015). Emulsion stabilization with Janus particles [PhD thesis]. University of Pennsylvania.

15. Fiberg, S. E., & Venable, R. (1983). Microemulsions. In P. Becher (Ed.), Encyclopedia of emulsion technology (Vol. 1). Marcel Dekker.

16. Solans, C., Pons, R., & Kunieda, H. (1997). Overview of basic aspects of microemulsions. In C. Solans & H. Kunieda (Eds.), Industrial applications of microemulsions (Vol. 66). Marcel Dekker.

17. Solans, C., Izquierdo, P., Nolla, J., Azemar, N., & Garcia-Celma, M. (2005). Nano-emulsions. Current Opinion in Colloid & Interface Science.

18. Jouanny-Bouyer, E. (2011). Stabilisation d'émulsions d'intérêt pharmaceutique par des protéines et des polysaccharides [PhD thesis]. Université Paris-Sud 11.

19. Shinoda, K. (1967). The effect of phase volume on the phase inversion temperature of emulsions stabilized with non-ionic surfactants. Journal of Colloid and Interface Science.

20. Clausse, D., Daniel-David, D., Gomez, F., Komunjer, L., Pezron, I., Dalmazzone, C., & Noik, C. (2007). Emulsion stability and interfacial properties - Application to complex emulsions of industrial interest. In T. F. Tadros (Ed.), Colloid stability and application in pharmacy. Wiley-VCH.

21. Hou, C. (1997). Characterization of new yeast lipases. Journal of the American Oil Chemists' Society.

22. Zeidani, K. (2007). Heavy oil-in-water emulsion flow and blocking mechanism in porous media [PhD thesis]. ProQuest.

23. Zaki, N. N., Carbonell, R. G., & Kilpatrick, P. K. (2003). Ind Eng Chem Res, 42, 6661–6672.

24. Schramm, L. L. (1992). Adv Chem Ser, 321, 1–51.

25. Mat, H., Samsuri, A., Rahman, W., & Rani, S. (2006). Research Paper, Department of Chemical Engineering, Universiti Teknologi Malaysia.

26. Mehta, S. D. (2006). Making and breaking of water in crude oil emulsions [PhD thesis]. Texas A&M University.

27. Davis, H. (1994). Colloids Surf A Physicochem Eng Asp, 91, 9–24.

28. Hasan, S. W., Ghannam, M. T., & Esmail, N. (2010). Fuel, 89, 1095–1100.

29. Ashrafizadeh, S., & Kamran, M. (2010). J Petrol Sci Eng, 71, 205–211.

30. Lin, C. Y., & Chen, L. W. (2006). Fuel Process Technol, 87, 309–317.

31. Alwadani, M. S. (2009). Characterization and rheology of water-in-oil emulsion from deepwater fields [PhD thesis]. Rice University.

32. Ilkhaani, S. (2009). Modeling and optimization of crude oil desalting [PhD thesis]. University of Waterloo.

33. Brochette, P. (1996). Formulation des émulsions et des microémulsions. Les Cahiers «Formulation et Formation», 7, 62–89.

34. Bendjaballah, M., Canselier, J. P., & Oumeddour, R. (2010). Optimization of oil-in-water emulsion stability: Experimental design, multiple light scattering, and acoustic attenuation spectroscopy. Journal of Dispersion Science and Technology, 31(9), 1260–1272.

35. El Hijri, J. (2008). Contribution expérimentale et numérique à l'étude de la remise en suspension des particules par l'activité humaine [PhD thesis]. Université de La Rochelle.

36. Jones, T. J., Neustadter, E. L., & Whittingham, K. P. (1978). Water-in-crude oil emulsion stability and emulsion destabilization by chemical demulsifiers. Journal of Canadian Petroleum Technology, 17, 100–108.

37. Yonguep, E., Kapiamba, F. K., Kabamba, K. J., & Chowdhury, M. (2022). Formation, stabilization and chemical demulsification of crude oil-in-water emulsions: A review. Petroleum Research.

38. Al-Otaibi, M., et al. (2003). Experimental investigation of crude oil desalting and dehydration. Chemical Engineering Communications, 190(1), 65–82.

39. Fetter Pruneda, E., Borrell Escobedo, E. R., & Garfias Vázquez, F. J. (2005). Optimum temperature in the electrostatic desalting of Maya crude oil. Journal of the Mexican Chemical Society, 49(1), 14–19.

40. Sellami, M., Naam, R., & Temmar, M. (2016). Optimization of operating parameters of oil desalting in Southern Treatment Unit (HMD/Algeria). Journal of Petroleum & Environmental Biotechnology, 7(271), 2.

41. Chawla, M. L. (n.d.). Field desalting of wet crude in Kuwait. Kuwait Oil Co. Society of Petroleum Engineers. SPE 15711.

42. Mandal, K. K. (2005, April). Improve desalter control. Hydrocarbon Processing.

43. Kokal, S. (2005). Crude oil emulsions: A state-of-the-art review. Society of Petroleum Engineers. SPE 77497.

44. Petreco Bilectric Dehydrators and Desalters. Cameron Petreco Process Systems. Retrieved from http://www.c-a-m.com/content/products/product_detail.cfm?pid=2630

45. Natco Dual Polarity Dehydrators and Desalters. Natco Oil Treating Technologies. Retrieved from http://www.natcogroup.com/Content.asp?t=ProductPage&ProductID=100

46. AGAR Control. Retrieved from http://www.agarcorp.com

47. Ramkrishna, D. (2014). Population balance modeling: Current status and future prospects. Annual Review of Chemical and Biomolecular Engineering, 5, 123–146.

48. Tahouni, N., & Abbasi, M. (2023). Parametric optimization of a crude oil treatment unit via PBE and DE. Chemical Engineering Research and Design, 190, 20–32.

49. Eibeck, A., & Wagner, W. (2000). Stochastic particle methods for multidimensional PBEs. SIAM Journal on Scientific Computing, 22(3), 802–821.

50. Storn, R., & Price, K. (1997). Differential evolution – A simple and efficient heuristic for global optimization over continuous spaces. Journal of Global Optimization, 11(4), 341–359.

51. Das, S., & Suganthan, P. N. (2011). Differential evolution: A survey of the state-of-the-art. IEEE Transactions on Evolutionary Computation, 15(1), 4–31.

Supplementary Material

Supplementary Material

Table S1: Water-wash experiments

X_exp (%)	S_exp_wash (mg/L)	E_exp_wash (%)
1.0	230.0	6.12
2.0	210.0	14.29
3.0	190.0	22.45
4.0	160.0	34.69
5.0	130.0	46.94
6.0	100.0	59.18
7.0	80.0	67.35
8.0	70.0	71.43
9.0	65.0	73.47
10.0	60.0	75.51

Table S2: Demulsifier-dose experiments

Qd_exp (L/h)	S_exp_demo (mg/L)	E_exp_demo (%)
0.35	240.0	3.61
1.0	210.0	15.66
2.0	180.0	27.71
3.0	150.0	39.76
4.0	120.0	51.81
5.0	90.0	63.86

Table S3: Temperature experiments

T_exp (°C)	S_exp_temp (mg/L)	E_exp_temp (%)
64.0	261.0	0.0
66.0	220.0	15.71
68.0	180.0	31.03
70.0	11.0	95.79
72.0	11.0	95.79
74.0	11.0	95.79
76.0	11.0	95.79
78.0	11.0	95.79
80.0	11.0	95.79

Figure S4: DESALINING PROCESS DIAGRAM

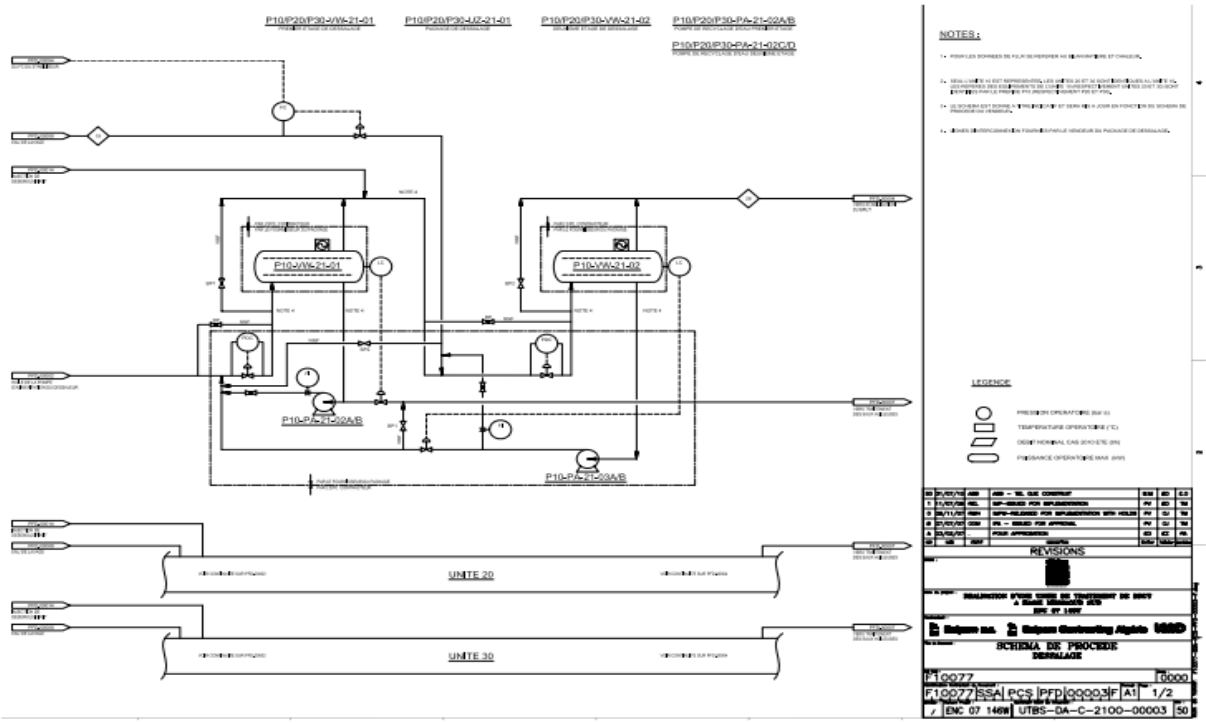

Figure S5: P&I DIAGRAM FIRST STAGE OF DESALINATION - UNIT 10